Supplementary Materials

Identification of differential and highly variable genes in cancer samples

The differentially expressed genes were identified by comparing the expression profiles between cancer samples and normal samples. For the expression data detected by the microarray technologies, the differentially expressed genes were identified using the SAM algorithm at FDR≤0.05 and fold change≥1.5. For the expression data detected by the high-through sequencing technology, we performed the differential expression analysis using R package DESeq at FDR≤0.05 and fold change≥1.5. The degree of expression variation was calculated by median absolute deviations (MAD), and the highly variable genes were considered as the genes within the top of 70%. Only genes that were differentially expressed and highly variable were used to build regulatory networks.

Partial least squares (PLS)

PLS finds the latent variables to fit the linear regression model between response variables exp_{G_i} and input variables including CN_{G_i}, $meth_{G_i}$, TF_j ($j=1,2\ldots,J$) and $miRNA_k$ ($k=1,2,\ldots,K$) by projecting the response variables and input variables to a new H dimension space.

$$X = TP^t + e$$

$$Y = Tb + f$$

where X represents a $N \times M$ matrix referring to N samples and M input variables, T represents a $N \times H$ matrix of X projection scores containing H latent variables (T_n, n=1……h), P represents the $H \times M$ orthogonal loading matrix of X, Y represents expression values of G_i in the N samples, b represents the regression coefficients of T, and e and f represent the random errors. The object of PLS is to maximize the covariance COV(Y,T_n). Then, based on the T, we estimated the regression coefficients of X on Y.

The data flow of CMDD when applied on GBM

CMDD was applied to the multi-dimensional datasets of 121 GBM samples including DNA mutation, copy number, methylation, gene expression, and miRNA expression profiles. By combining the DNA mutation and copy number data, 119 genes were observed to alter in at least 10 GBM samples, with 42 showing significant difference of gene expression (t-test, FDR≤0.05) as the candidate genes. Based on the GBM samples and 10 normal samples, 5083 differentially expressed genes were obtained using SAM (Fold change≥1.5 and FDR≤0.05), in which 4708 genes with high expression variation across GBM samples were selected to construct the dysregulated network. For each candidate gene, a dysregulated network was built (Supplementary Table S1). We found that different candidate genes induced the different numbers of dysregulated relationships from 589 to 1981, referring to 491 to 1364 genes. Considering the functional associations between the candidate genes and genes in the dysregulated networks, we selected genes that were within two-step distance from candidate genes in protein interaction networks as the dysregulated genes.

Analysis of expression correlation of dysregulated genes induced by core genes

To evaluate dysregulated genes induced by the module, we compared the expression correlation among the dysregulated genes with those of randomly selected genes. For each core gene, the randomly selected genes had the same size as its dysregulated genes. The random genes were selected as follows: Firstly, we randomly selected 17 genes in protein interaction network, and collected the neighbors of these 17 genes as a control gene set. Then, the random genes were randomly selected from the control gene set. The above procedures were repeated 100 times, and 100 random gene sets

were obtained. We found that that dysregulated genes induced by genes in the module tend to show significantly higher expression correlations compared to randomly selected genes (Supplementary Figure S4).

Detecting novel core genes in GBM

Some genes in the core module were rarely reported previously to be associated with GBM. In the core module, both *METTL1* and *CTDSP2*, with the highest degree of 13 were connected with 7 known GBM associated genes (Supplementary Figure S1). *CTDSP2* has been reported to play important roles in neuronal differentiation, neurogenesis and G1/S transition (1). The expression of *METTL1* can partially promote cell growth (2). However, little was known about their roles in GBM. Functions and pathways enriched by the dysregulated genes of *METTL1* exhibited high overlap with those of 7 known GBM associated genes (P=6.4×10^{-15} for pathways and P=1.2×10^{-78} for functions Supplementary Figure S2A). Furthermore, the cancer associated functions and pathways affected by *METTL1* were frequently enriched by dysregulated genes of 7 known genes, such as “cell differentiation”, “cell cycle” and “Glioma” pathway (Supplementary Figure S2B).

We noted that many dysregulated genes affected by *METTL1* have been reported to play key roles in cancers (Supplementary Figure S2C). For instance, caspase3, which is encoded by the dysregulated gene *CASP3*, can cleave and active protease to initiate apoptosis by extrinsic and intrinsic pathways in response to apoptotic stimuli (3). The dysregulated interaction between miR-138 and *CASP3* in our finding can be partially explained by a previous report that miR-138 can influence *CASP3* expression (4). *MAPK1* (5), *CDKN2A* (6), *AKT1* (7) and *BRCA1*(8), were well-known to influence a variety of tumor biological behaviors, suggesting a potential role of *METTL1* in tumorigenesis.

To determine whether the alteration and expression of *METTL1* are associated with survival, the GBM patients were divided into two groups (*METTL1* alteration vs *METTL1* non-alteration). We found that the patients with *METTL1* alteration had poor

prognosis (*P*=0.015, log-rank test, Supplementary Figure S2D). Based on the expression of *METTL1*, we grouped the patients into a high-risk group (expression in top 25%), a low-risk group (expression in bottom 25%) and a moderate-risk (the remainder of the patients). There was a significant difference in overall survival for the 3 groups (*P*=0.0015, log-rank test, Supplementary Figure S2E). High expression of *METTL1* was associated with poor survival. An independent dataset GSE4412 (9) showed consistently significant survival difference for the 3 groups (*P*=0.03, log-rank test, Supplementary Figure S2F).

Similar results were obtained for *CTDSP2*. We found that the functions and pathways significantly enriched by the dysregulated genes of *CTDSP2* were also frequently overlapped by those of 7 known GBM associated genes (Supplementary Figure S3A), such as cell cycle, Jak-STAT signaling pathway and MAPK signaling pathway (Supplementary Figure S3B). Meanwhile, we found that many of the dysregulated genes affected by *CTDSP2* have been reported to play key roles in cancers (Supplementary Figure S3C). For example, *CCND1* is a crucial regulator for G1 to S phase transition in cell cycle(10), and *CTDSP2* might indirectly contribute to cell cycle disorder through dysregulation of transcription factors *STAT5B* and *ATF-2* on the *CCND1* expression(11). Furthermore, we analyzed whether the genetic alteration and expression of *CTDSP2* are associated with GBM survival. The results showed that the patients with *CTDSP2* alteration had poor prognosis (*P*=0.07, log-rank test, Supplementary Figure S3D), and high expression of *CTDSP2* was also associated with poor survival (*P*=0.025, log-rank test, Supplementary Figure S3E). Moreover, an independent dataset GSE4412 further showed consistent prognostic effect of *CTDSP2* (*P*=0.09, log-rank test, Supplementary Figure S3F).

These findings suggested that *METTL1* and *CTDSP2* were the potential novel genes whose genetic alterations may contribute to the development of GBM. They could indirectly participate in pathogenesis by inducing dysregulation of crucial response genes.

1. Zhu, Y., Lu, Y., Zhang, Q., Liu, J.J., Li, T.J., Yang, J.R., Zeng, C. and Zhuang, S.M. (2012) MicroRNA-26a/b and their host genes cooperate to inhibit the G1/S transition by activating

the pRb protein. *Nucleic Acids Res*, **40**, 4615-4625.

2. Cartlidge, R.A., Knebel, A., Peggie, M., Alexandrov, A., Phizicky, E.M. and Cohen, P. (2005) The tRNA methylase METTL1 is phosphorylated and inactivated by PKB and RSK in vitro and in cells. *EMBO J*, **24**, 1696-1705.
3. Xiao, L.J., Zhao, S., Zhao, E.H., Zheng, X., Gou, W.F., Takano, Y. and Zheng, H.C. (2013) Clinicopathological and prognostic significance of Ki-67, caspase-3 and p53 expression in gastric carcinomas. *Oncol Lett*, **6**, 1277-1284.
4. He, S., Liu, P., Jian, Z., Li, J., Zhu, Y., Feng, Z. and Xiao, Y. (2013) miR-138 protects cardiomyocytes from hypoxia-induced apoptosis via MLK3/JNK/c-jun pathway. *Biochem Biophys Res Commun*, **441**, 763-769.
5. Grieco, L., Calzone, L., Bernard-Pierrot, I., Radvanyi, F., Kahn-Perles, B. and Thieffry, D. (2013) Integrative modelling of the influence of MAPK network on cancer cell fate decision. *PLoS Comput Biol*, **9**, e1003286.
6. Kawamata, N., Morosetti, R., Miller, C.W., Park, D., Spirin, K.S., Nakamaki, T., Takeuchi, S., Hatta, Y., Simpson, J., Wilcyznski, S. *et al.* (1995) Molecular analysis of the cyclin-dependent kinase inhibitor gene p27/Kip1 in human malignancies. *Cancer Res*, **55**, 2266-2269.
7. Chakravarti, A., Loeffler, J.S. and Dyson, N.J. (2002) Insulin-like growth factor receptor I mediates resistance to anti-epidermal growth factor receptor therapy in primary human glioblastoma cells through continued activation of phosphoinositide 3-kinase signaling. *Cancer Res*, **62**, 200-207.
8. Etemadmoghadam, D., Weir, B.A., Au-Yeung, G., Alsop, K., Mitchell, G., George, J., Davis, S., D'Andrea, A.D., Simpson, K., Hahn, W.C. *et al.* (2013) Synthetic lethality between CCNE1 amplification and loss of BRCA1. *Proc Natl Acad Sci U S A*, **110**, 19489-19494.
9. Freije, W.A., Castro-Vargas, F.E., Fang, Z., Horvath, S., Cloughesy, T., Liau, L.M., Mischel, P.S. and Nelson, S.F. (2004) Gene expression profiling of gliomas strongly predicts survival. *Cancer Res*, **64**, 6503-6510.
10. Tashiro, E., Tsuchiya, A. and Imoto, M. (2007) Functions of cyclin D1 as an oncogene and regulation of cyclin D1 expression. *Cancer science*, **98**, 629-635.
11. Oleaga, C., Ciudad, C.J., Noe, V. and Izquierdo-Pulido, M. (2012) Coffee polyphenols change the expression of STAT5B and ATF-2 modifying cyclin D1 levels in cancer cells. *Oxidative medicine and cellular longevity*, **2012**, 390385.

Supplementary Figure Legends

Supplementary Figure S1

The degree of member genes in the core module. Red bar represent the number of connections of genes with known GBM-associated member gene, while gray bar represent the degree with the rest member genes.

Supplementary Figure S2

The association of METTL1 with GBM. (A) The overlap of pathways (top) and functions (bottom) affected by METTL1 and 7 GBM genes through dysregulated genes. (B) The cancer associated pathways and functions enriched by the dysregulated genes of METTL1 are frequently affected by 7 known GBM associated genes. (C) The dysregulated network of METTL1. Dysregulated genes are colored byblue. (D) Kaplan–Meier estimates of overall survival for TCGA GBM patients with or without METTl1 alteration. (E) Kaplan–Meier estimates of overall survival using METTL1 expression in TCGA data sets. (F) Kaplan–Meier estimates of overall survival using METTL1 expression in GSE4412 data sets.

Supplementary Figure S3

The association of CTDSP2 with GBM. (A) The overlap of pathways (top) and functions (bottom) affected by CTDSP2 and 7 GBM genes through dysregulated genes. (B) The cancer associated pathways enriched by the dysregulated genes of CTDSP2 are frequently affected by 7 known GBM associated genes. (C) The dysregulated network of CTDSP2. Dysregulated genes are colored by blue. (D) Kaplan–Meier estimates of overall survival for TCGA GBM patients with or without CTDSP2 alteration. (E) Kaplan–Meier estimates of overall survival using CTDSP2 expression in TCGA data sets. (F) Kaplan–Meier estimates of overall survival using CTDSP2 expression in GSE4412 data sets.

Supplementary Figure S4

The cumulative distribution of expression correlation coefficients of dysregulated genes (red) for 17 genes in the module compared with that of 100 random selected gene sets with same size (gray), which were connected to 17 randomly selected genes in the protein interaction network (Kolmogorov-Smirnov test) .

Supplementary Figure S5

The overlap between functions annotated by member genes (left) and functions enriched by their dysregulated genes (right) (hyper-geometric test).

Supplementary Figure S6

The number of dysregulated genes with degree above 7 in the comprehensive network. Bars with dark gray show the number of cancer associated genes that appear in OMIM, CGC or GAD.

Supplementary Figure S7

Kaplan–Meier estimates of overall survival are shown for GBM patients in TCGA using the expression of ESR1. The chocolate curve and cyan curve represent ESR1 higher expression (top 50%) and lower expression (bottom 50%), respectively.

Supplementary Figure S8

The detailed dysregulation of dysregulated genes induced by genes in the module in the biological process of “glial cell differentiation”; ”apoptotic signaling pathway” and ”MAPK cascade”.

Supplementary Figure S9

Comprehensive analysis of core modules in OV. (A) The core gene modules in OV. (B) The biological functions and pathways significantly enriched by the core modules. (C) Comprehensive dysregulated network induced by core modules. (D) Contributions of different regulators in the dysregulated network affected by member genes.

Supplementary Figure S10

Comprehensive analysis of core modules in HNSC. (A) The core gene modules in HNSC. (B) The biological functions and pathways significantly enriched by the core modules. (C) Comprehensive dysregulated network induced by core modules. (D) Contributions of different regulators in the dysregulated network affected by member genes. (E) Some survival associated clique modules in HNSC.

Supplementary Figure S11

Comprehensive analysis of core modules in LUAD. (A) The core gene modules in LUAD. (B) The biological functions and pathways significantly enriched by the core modules. (C) Comprehensive dysregulated network induced by core modules. (D) Contributions of different regulators in the dysregulated network affected by member genes. (E) Some survival associated clique modules in LUAD.

Supplementary Figure S12

Comprehensive analysis of core modules in CESC. (A) The core gene modules in CESC. (B) The biological functions and pathways significantly enriched by the core modules. (C) Comprehensive dysregulated network induced by core modules. (D) Contributions of different regulators in the dysregulated network affected by member genes. (E) Some survival associated clique modules in CESC.

Supplementary Figure S13

Comprehensive analysis of core modules in BRCA. (A) The core gene modules in BRCA. (B) The biological functions and pathways significantly enriched by the core modules. (C) Comprehensive dysregulated network induced by core modules. (D) Contributions of different regulators in the dysregulated network affected by member genes. (E) Some survival associated clique modules in BRCA.

Supplementary Figure S14

Comprehensive analysis of core modules in PRAD. (A) The core gene modules in PRAD. (B) The biological functions and pathways significantly enriched by the core modules. (C) Comprehensive dysregulated network induced by core modules. (D) Contributions of different regulators in the dysregulated network affected by member genes.

Supplementary Figure S15

Some survival associated clique modules in OV. (A) The survival association of four modules in OV (B) The combined prognostic effect of alterations of genes in the two modules, respectively. One module contained PUDF60, SOX18, CCDC88A, MED4 and THOC7, the other contained LDHB, MRPS22 and ATP5C1.

Supplementary Figure S16

A clique module (ARNT, NFE2L2, BARD1, SUB1, ATF2, PTEN and TOPBP1) contained genes with different prognostic effect in HNSC. (A) Two subgroups identified by applying unsupervised hierarchical clustering to HNSC samples with alterations of at least one gene in the module. Red represents subgroup1 and blue subgroup2. (B) Two subgroups showed different prognosis. (C) Two subgroups and HNSC samples without any alteration of the module (Non-alteration group) showed different prognosis. (D) Survival analysis between subgroup1 and Non-alteration group. (E) Survival analysis between subgroup2 and Non-alteration group.

Supplementary Figure S17

A clique module (TAF9, HOXB7, EEF1D and RXRB) contained genes with different prognostic effect in OV. (A) Two subgroups identified by applying unsupervised hierarchical clustering to OV samples with alterations of at least one gene in the module. Red represents subgroup1 and blue subgroup2. (B) Two subgroups showed different prognosis. (C) Two subgroups and OV samples without any alteration of the module (Non-alteration group) showed different prognosis. (D) Survival analysis between subgroup1 and Non-alteration group. (E) Survival analysis between subgroup2 and Non-alteration group.

Supplementary Figure S18

A clique module (MED21, MYC, ZHX1, KPNA2 and USF2) contained genes with different prognostic effect in LUAD. (A) Two subgroups identified by applying unsupervised hierarchical clustering to LUAD samples with alterations of at least one gene in the module. Red represents subgroup1 and blue subgroup2. (B) Two subgroups showed different prognosis. (C) Two subgroups and LUAD samples without any alteration of the module (Non-alteration group) showed different prognosis. (D) Survival analysis between subgroup1 and Non-alteration group. (E) Survival analysis between subgroup2 and Non-alteration group.

Supplementary Figure S19

Comparisons of the core modules and their dysregulated genes among seven types of cancer.

Supplementary Figure S20

Comparison of EGFR-associated regulatory networks between multi-omics data and 9 different combinations. (A) The heatmap of regulatory network identified by multi-omics data. (B) The number of regulatory relationships identified from multi-omics data and 9 different combinations. (C) The overlap of regulated genes in regulatory networks between multi-omics data and other different combinations.

Supplementary Figure S21

Comparison of core modules identified by multi-omics data and 9 different combinations with only two or three types of data. (A) The heatmap of member genes identified from multi-omics data and 9 different combinations. (B) The modules identified from 4 different combinations.

Supplementary Figure S1

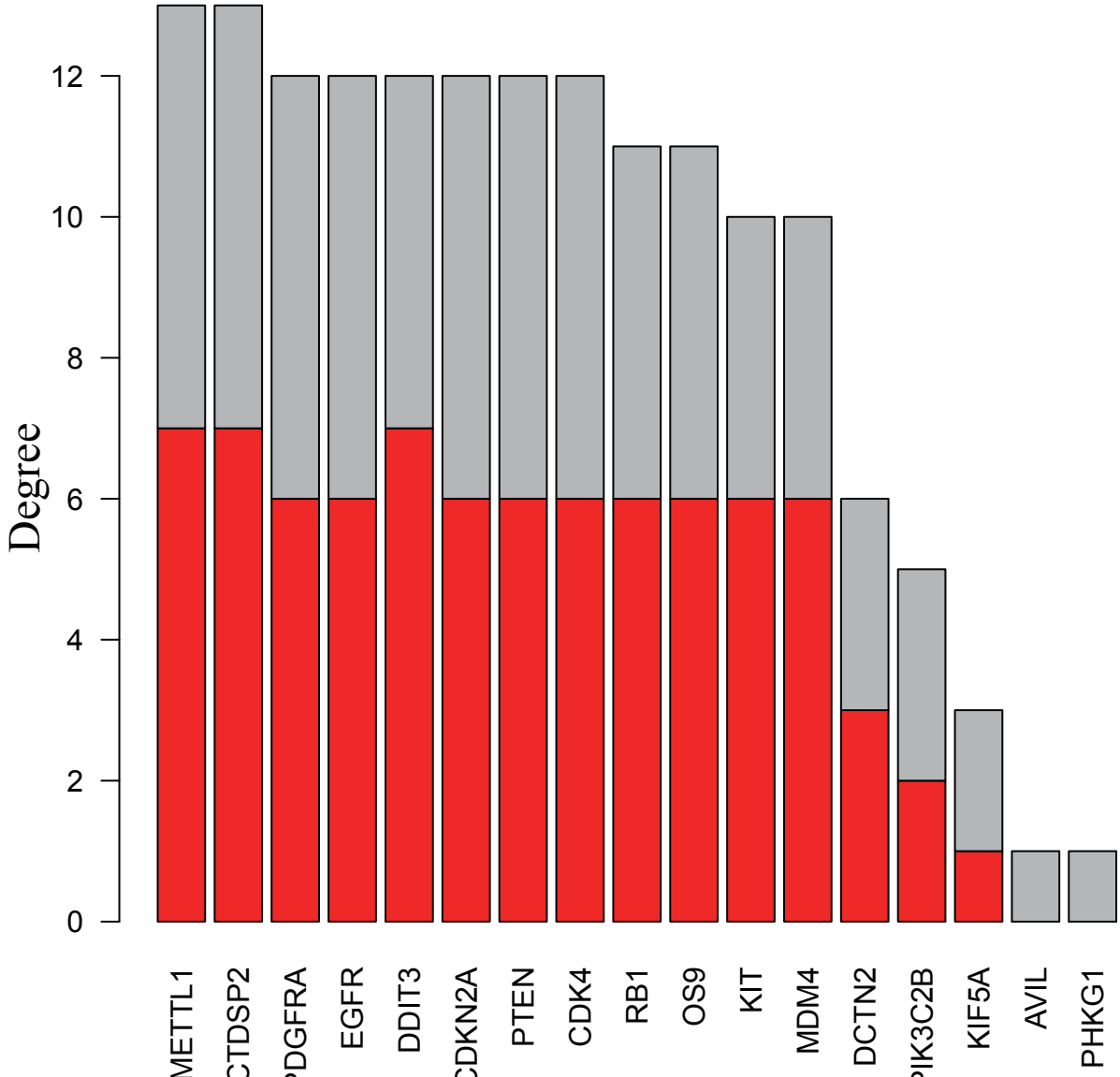

Supplementary Figure S2

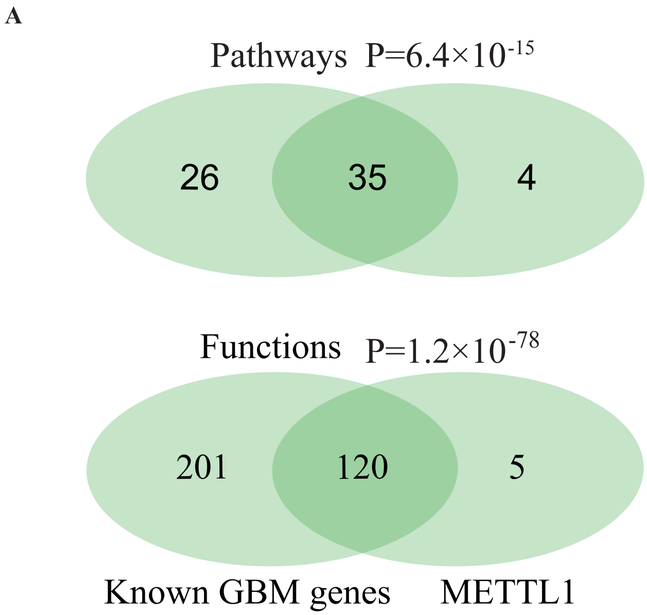

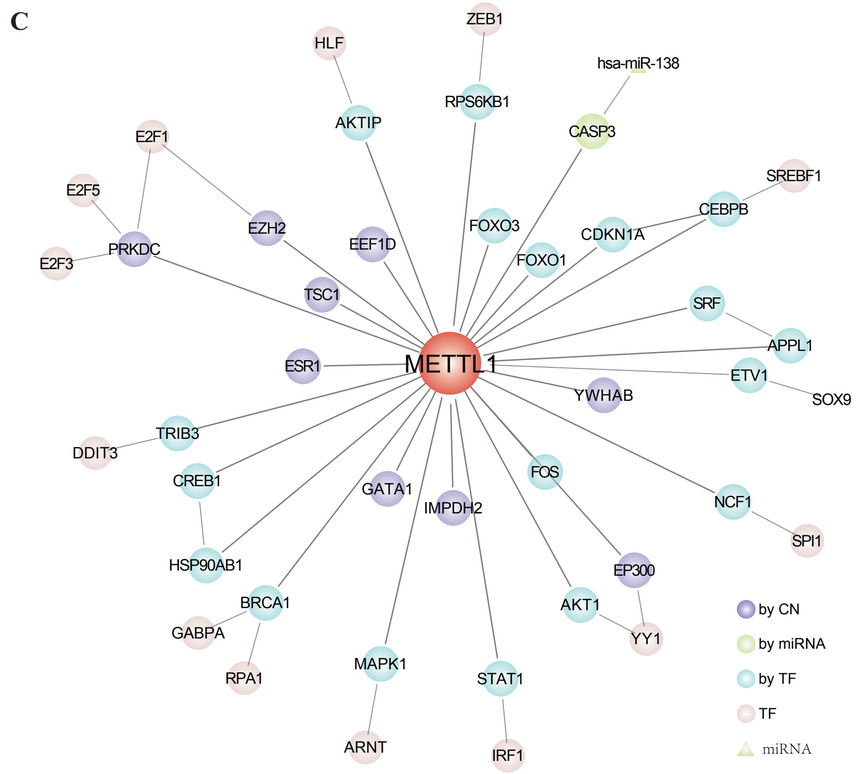

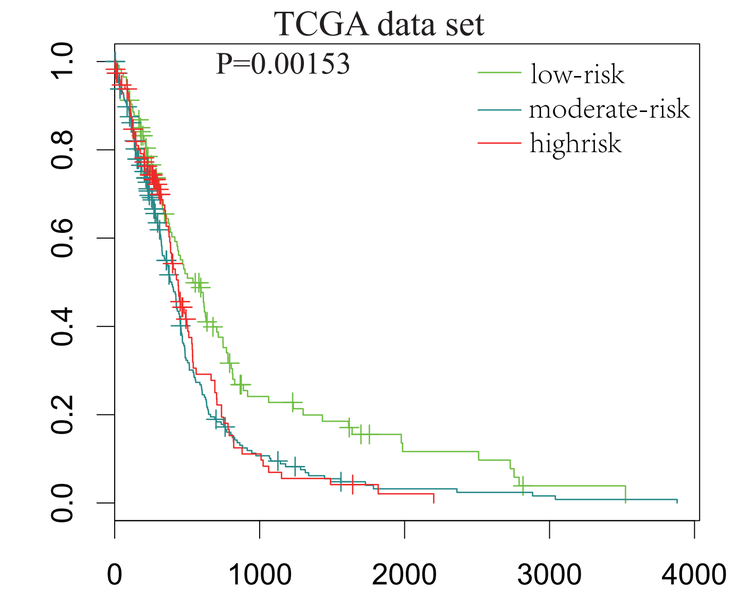

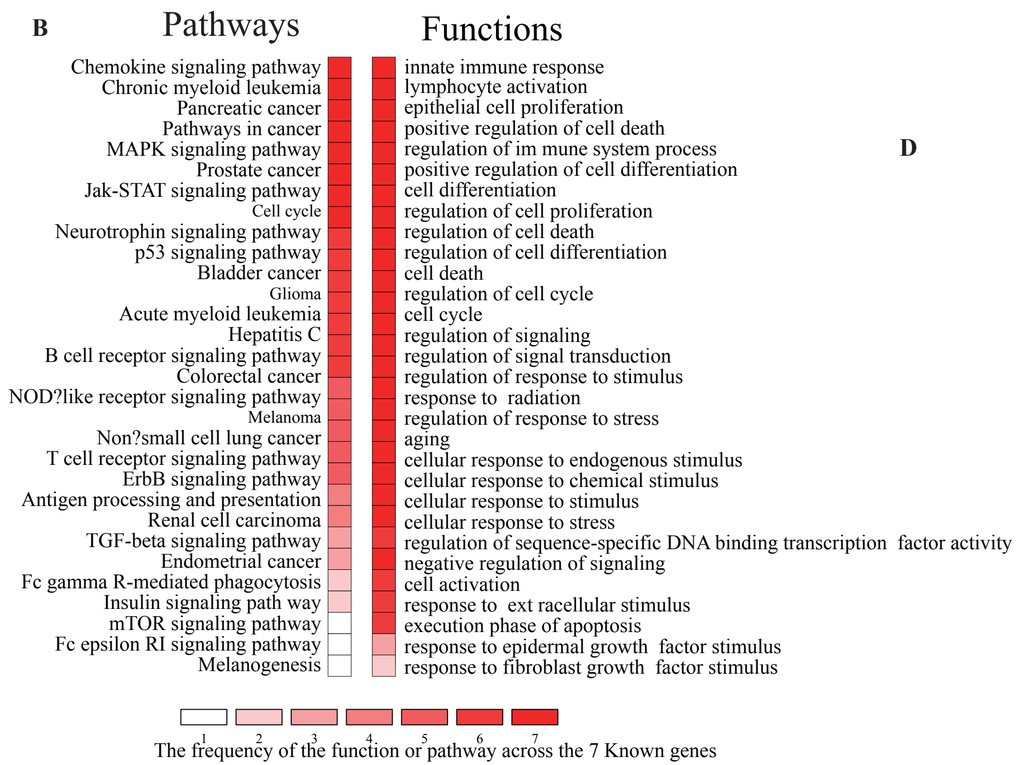

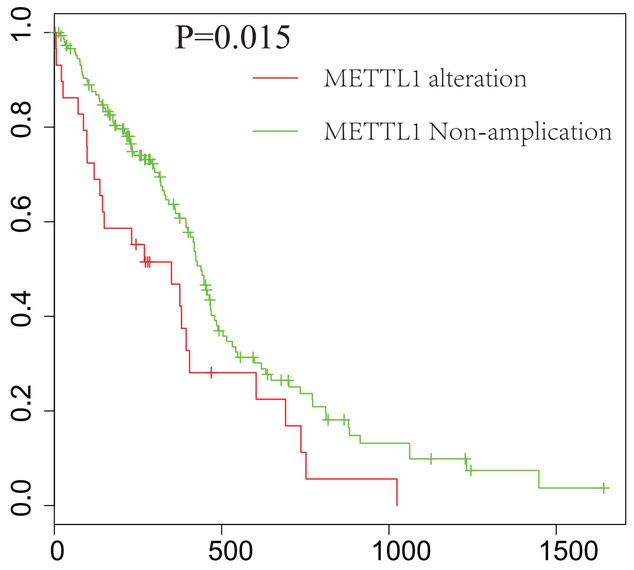

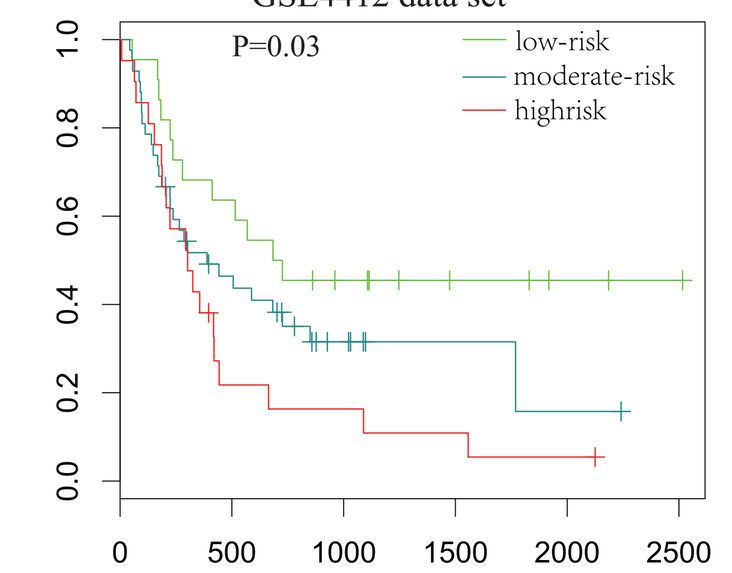

Supplementary Figure S3

A

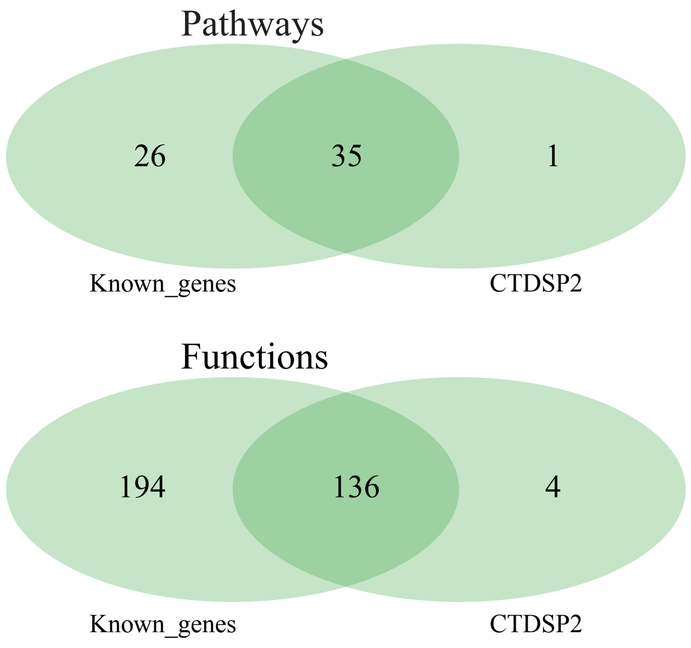

B

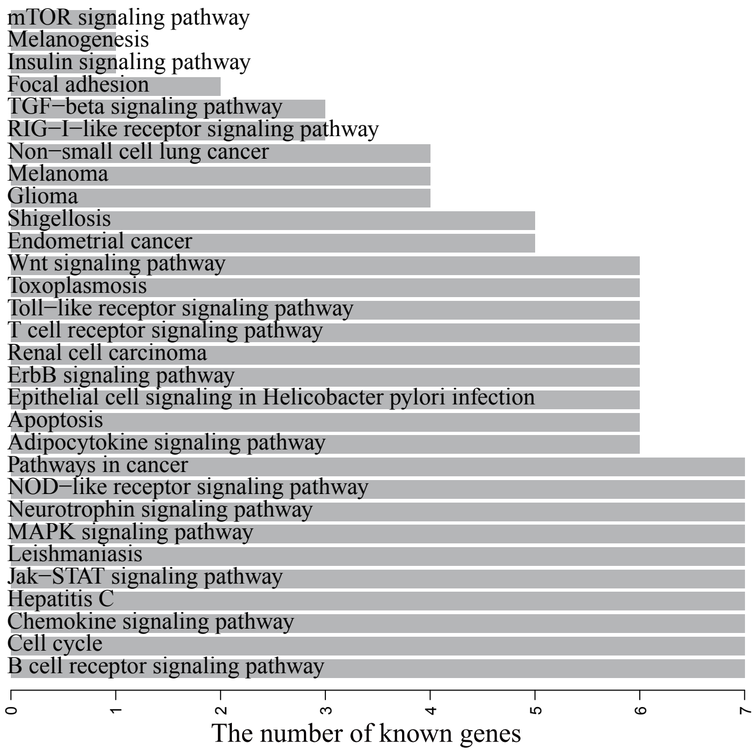

C

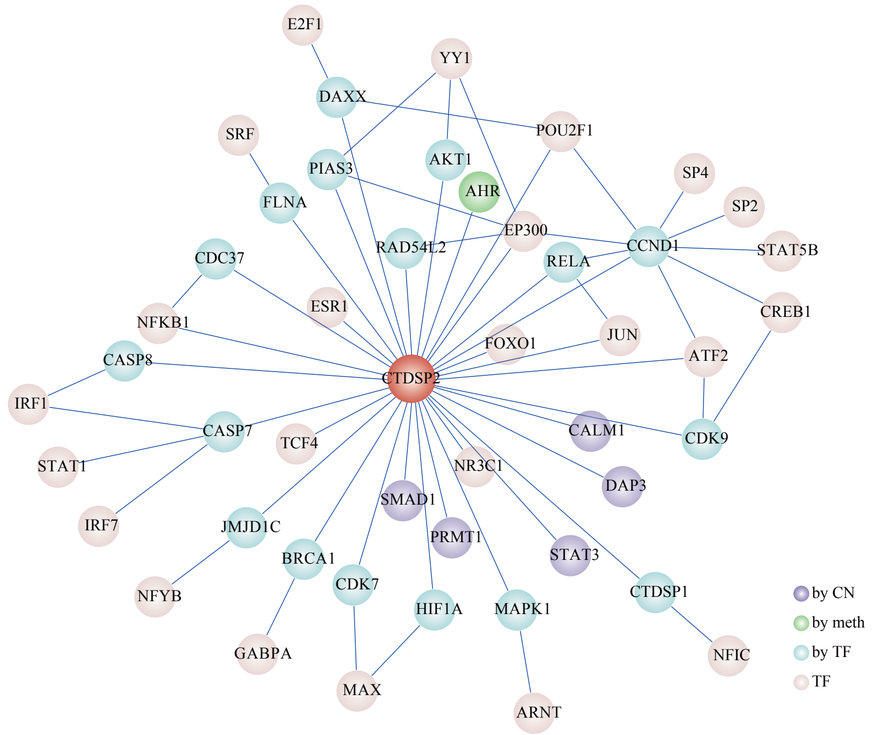

D

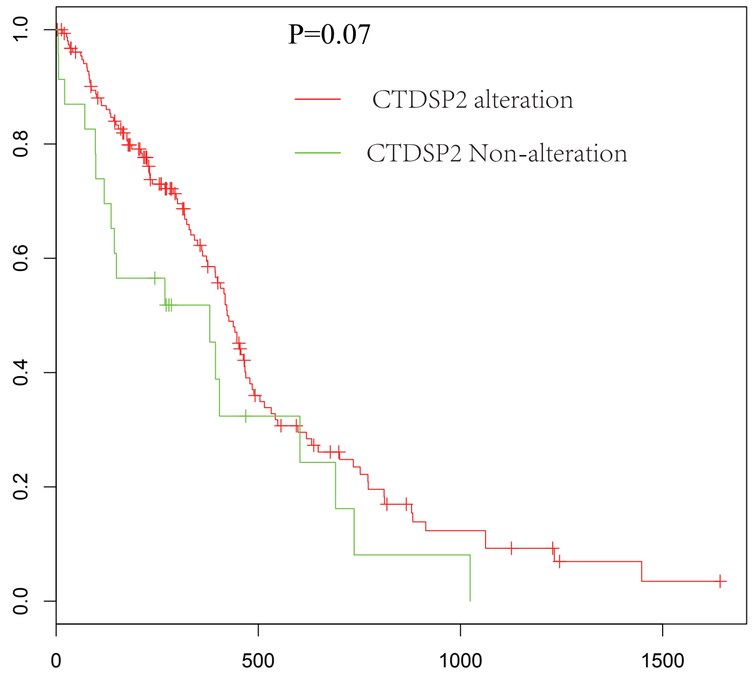

E

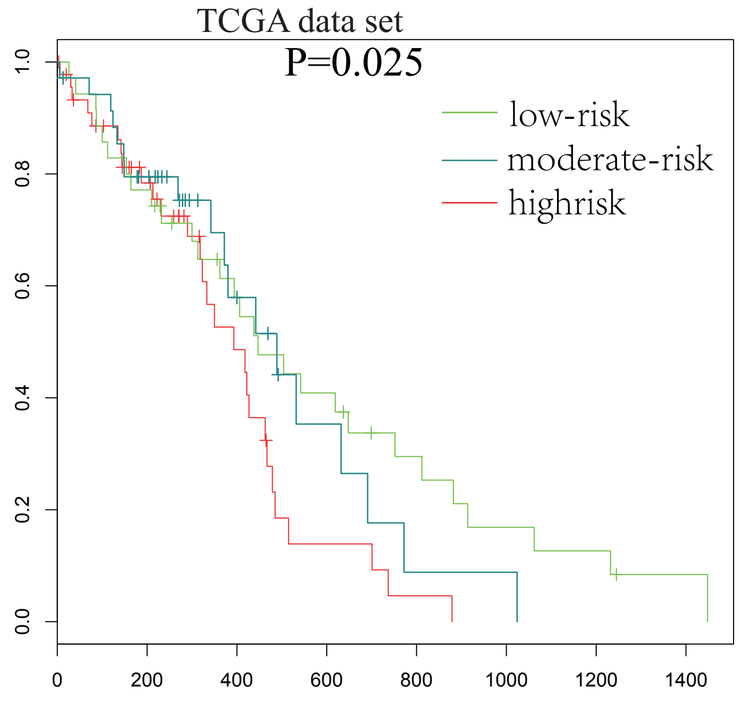

F

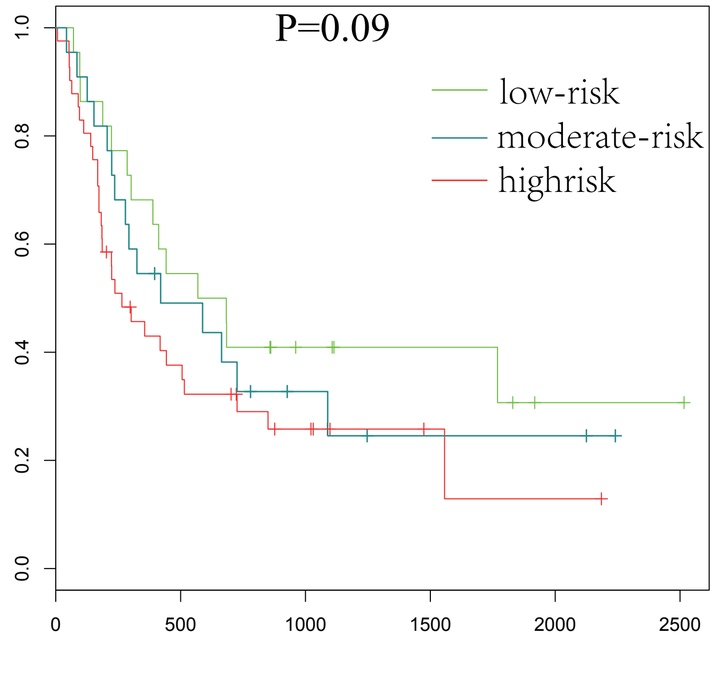

Supplementary Figure S4

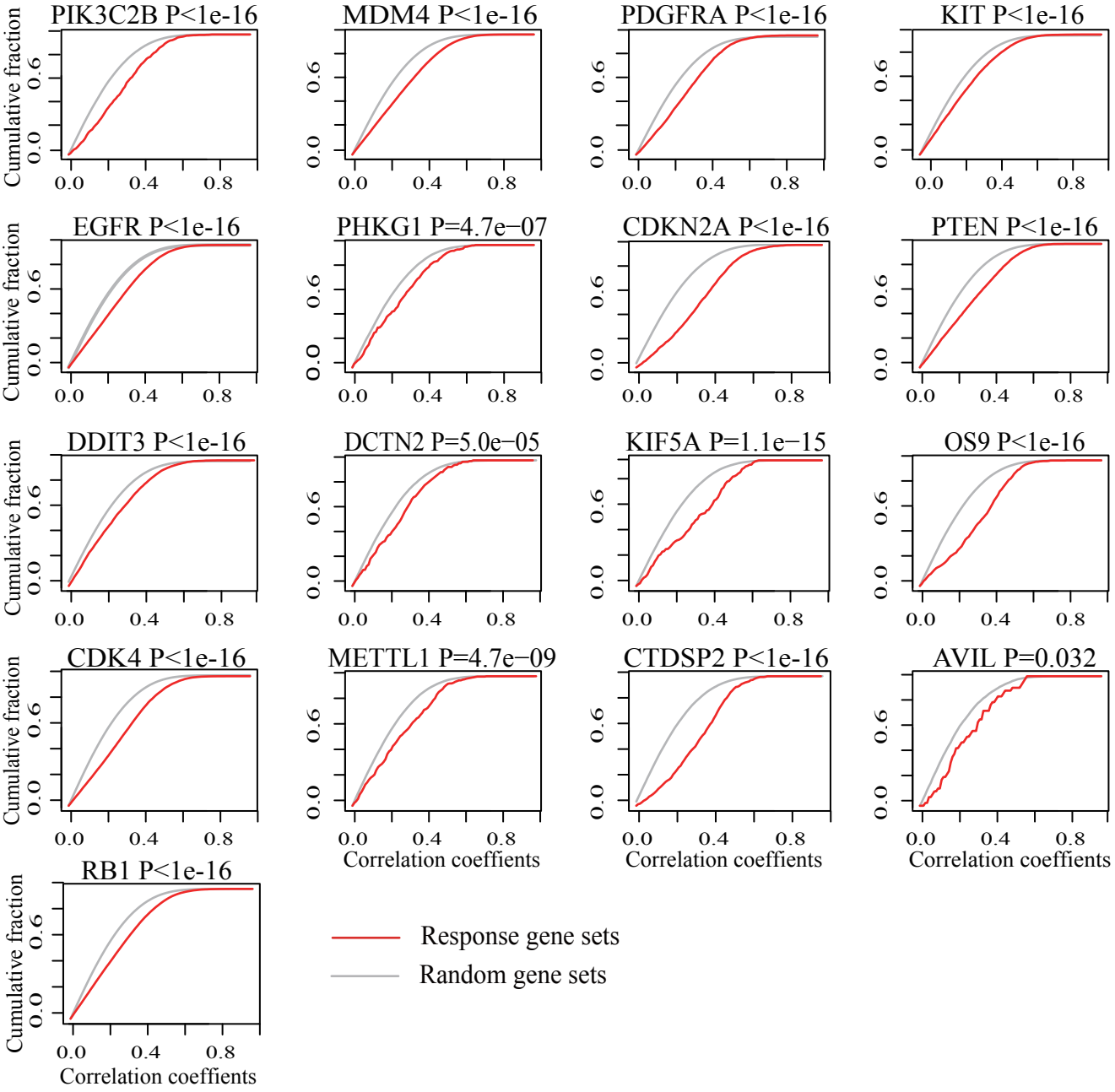

Supplementary Figure S5

PIK3C2B

P=0.08

MDM4

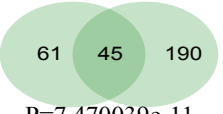

P=7.470039e-11

PDGFRA

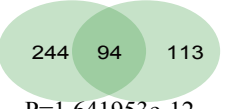

P=1.641953e-12

KIT

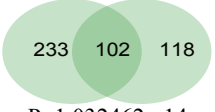

P=1.032462e-14

EGFR

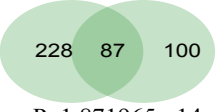

P=1.871965e-14

PHKG1

P=0.851014

CDKN2A

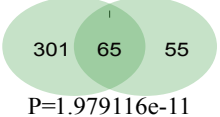

P=1.979116e-11

PTEN

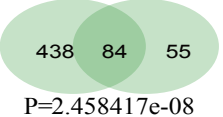

P=2.458417e-08

DDIT3

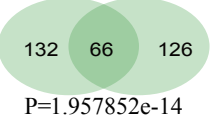

P=1.957852e-14

DCTN2

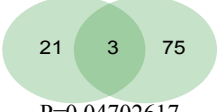

P=0.04702617

KIF5A

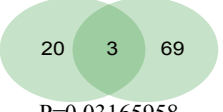

P=0.03165958

OS9

P=0.1027450

CDK4

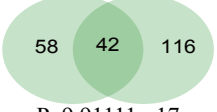

P=9.91111e-17

METTL1

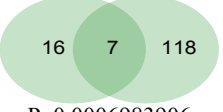

P=0.0006983906

AVIL

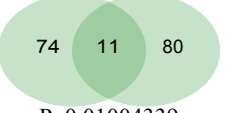

P=0.01004339

CTDSP2

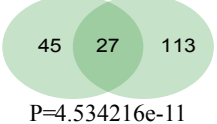

P=4.534216e-11

RB1

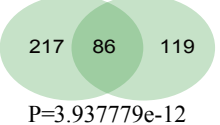

P=3.937779e-12

Supplementary Figure S6

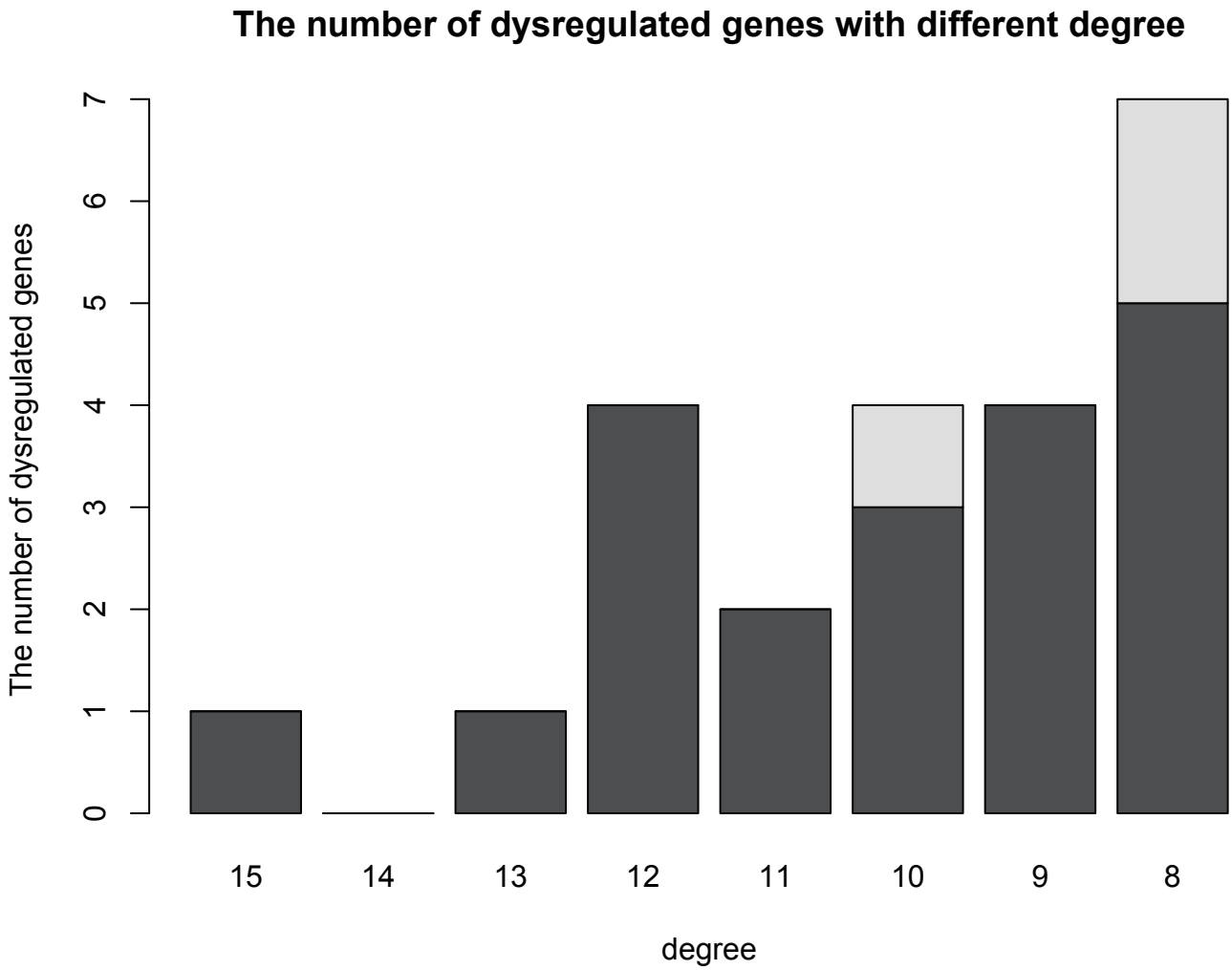

Supplementary Figure S7

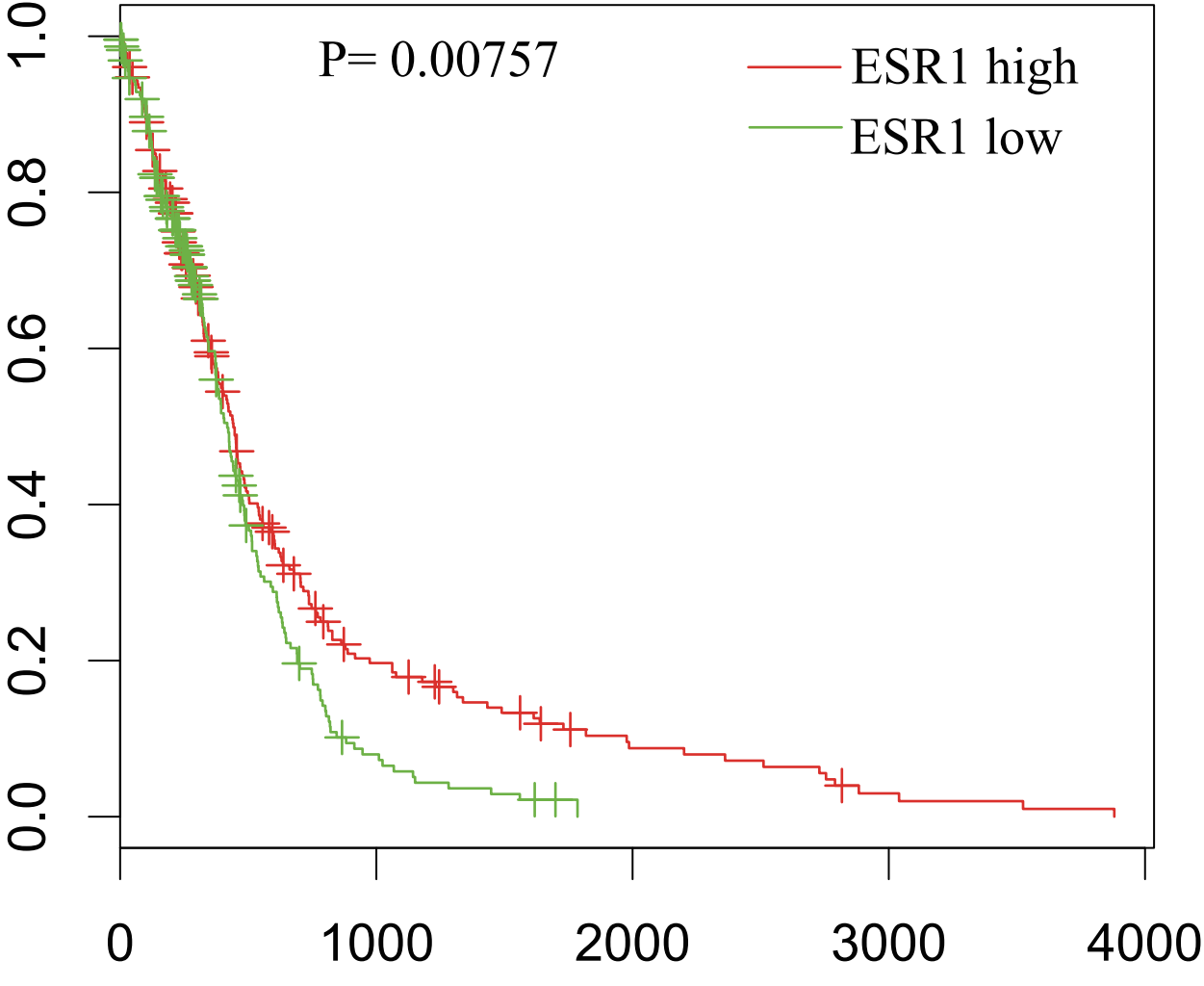

Supplementary Figure S8

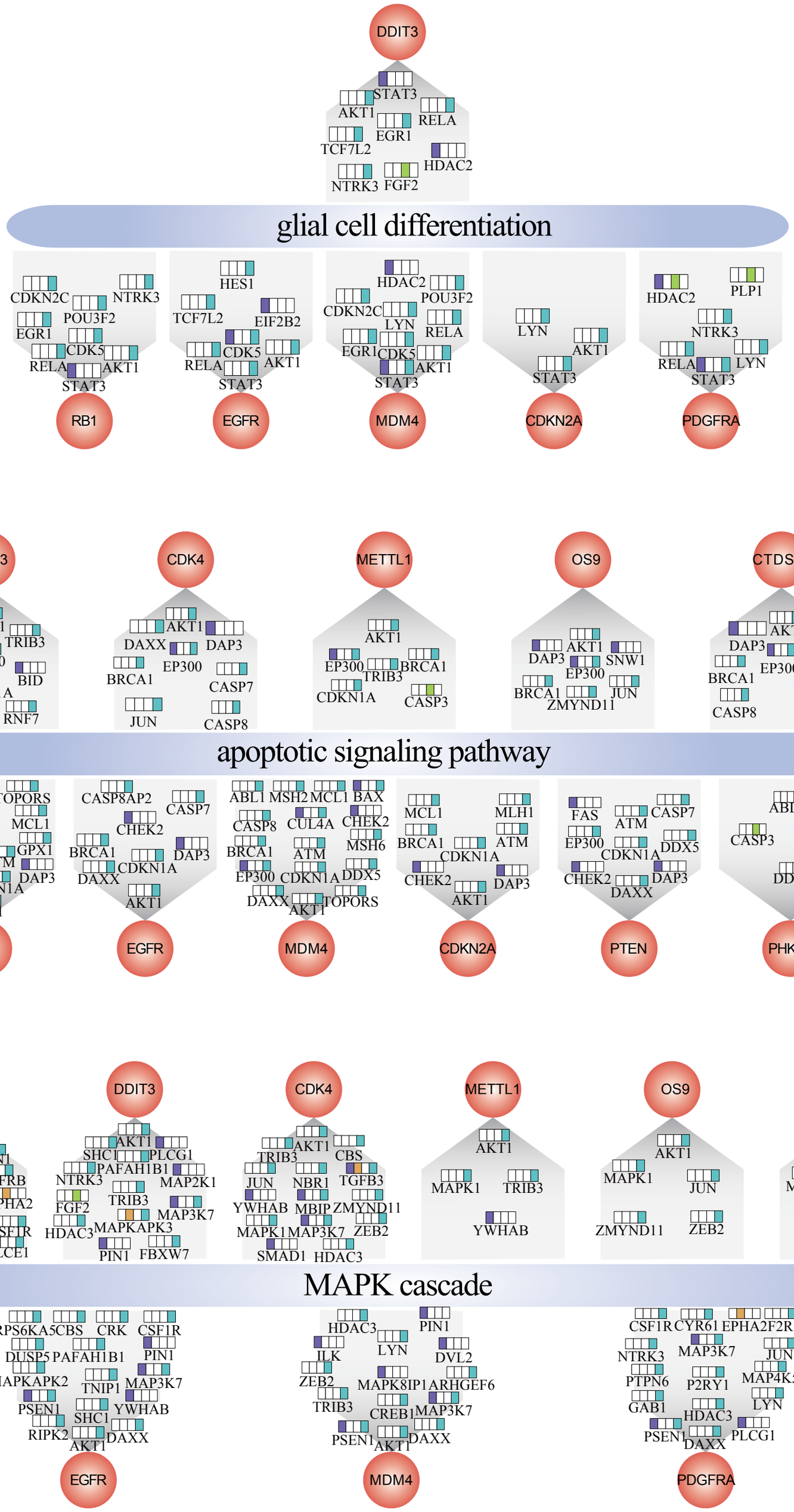

Supplementary Figure S9

A

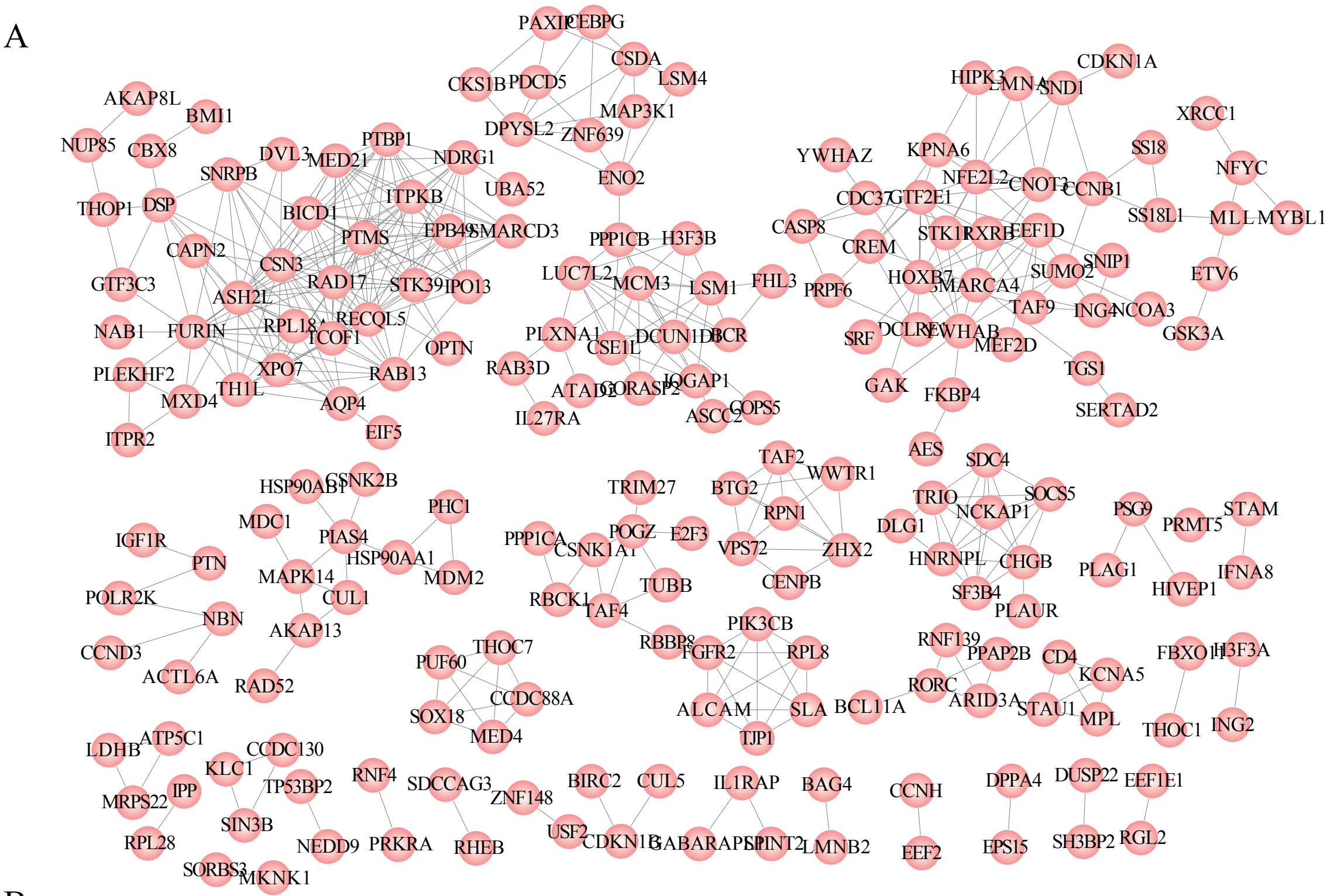

B

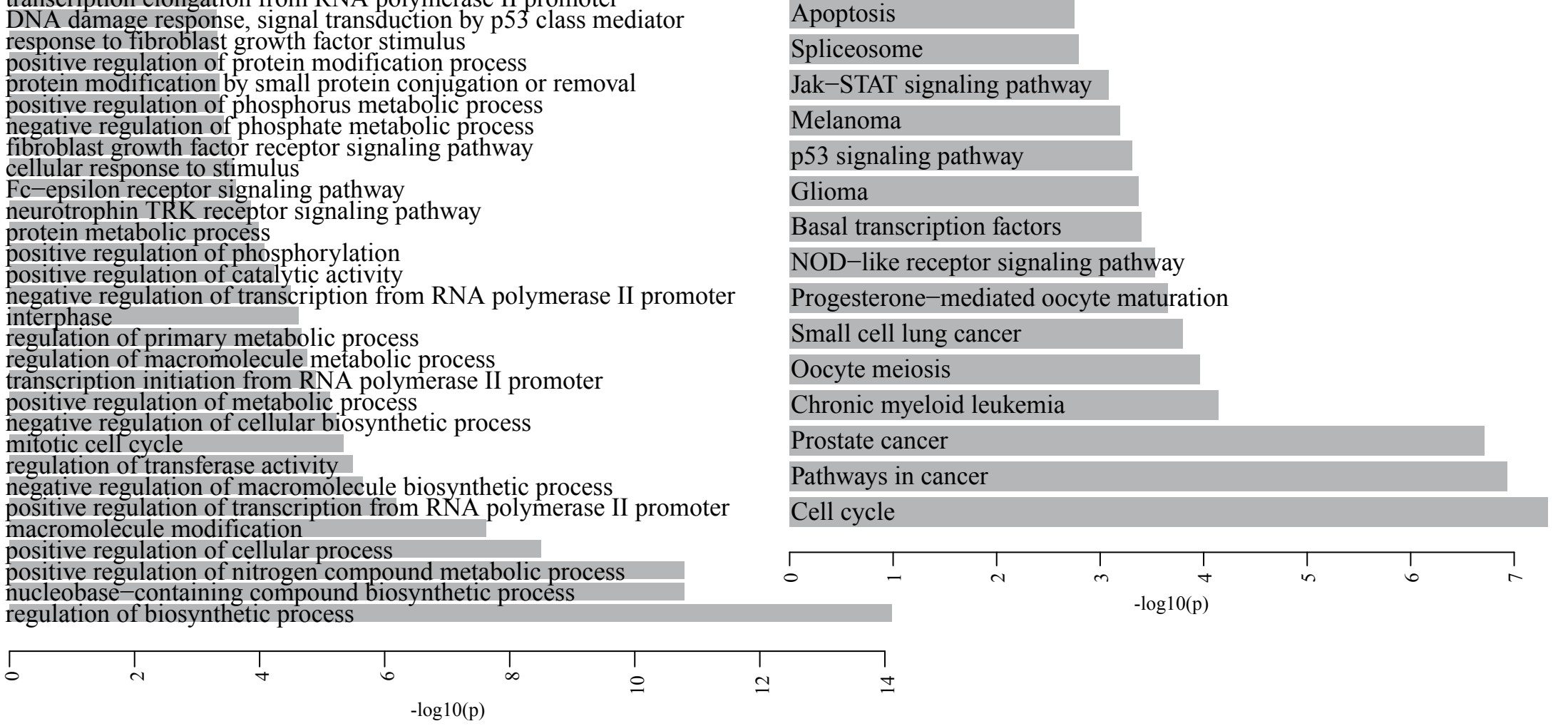

C

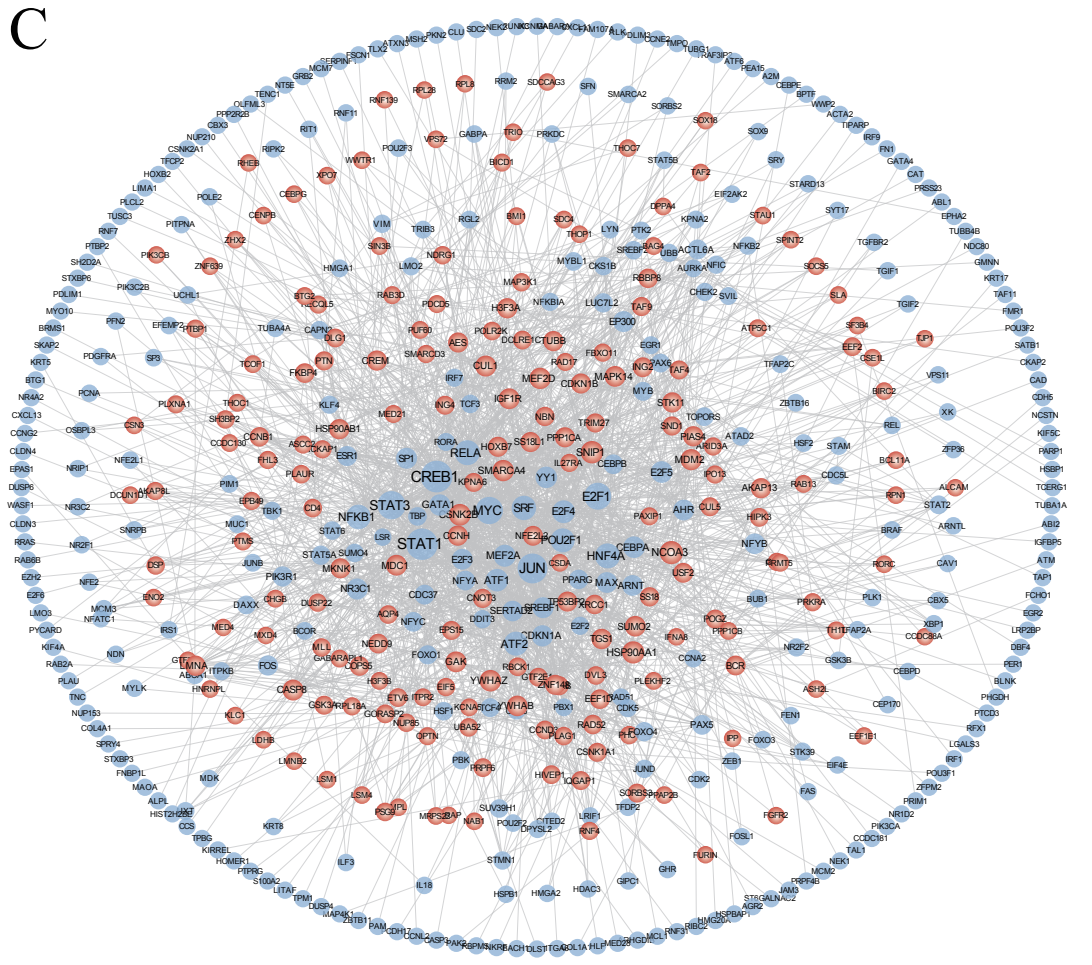

D

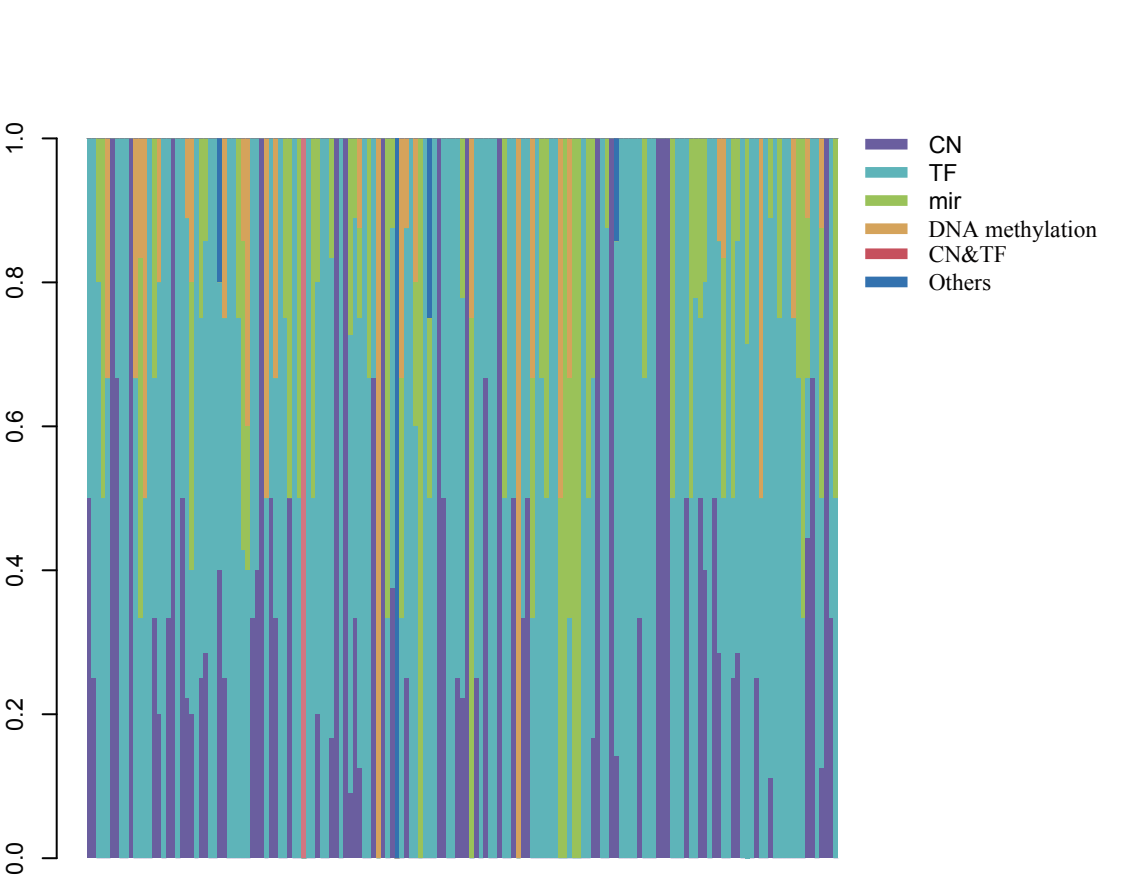

Supplementary Figure S10

A

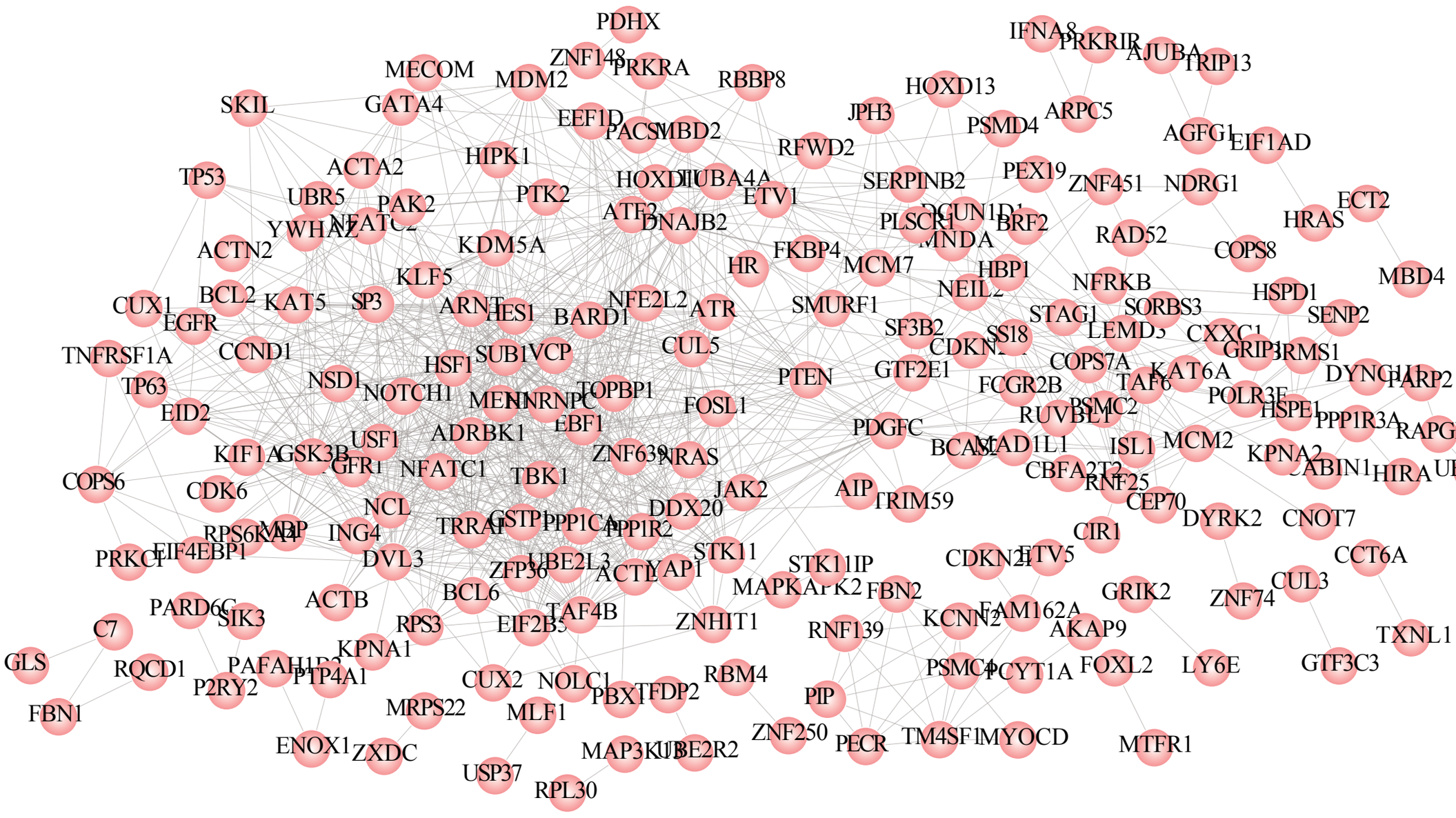

B

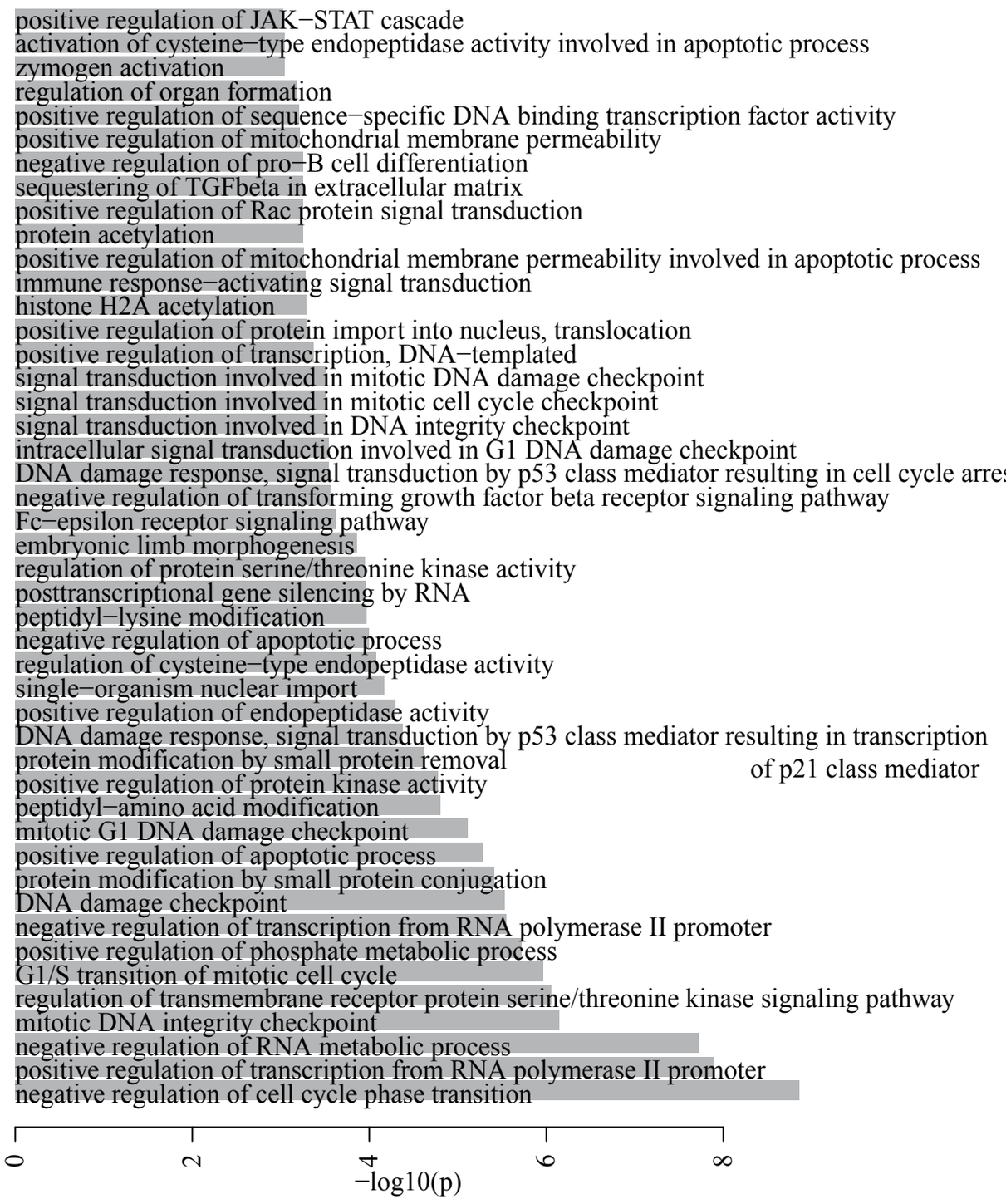

C

D

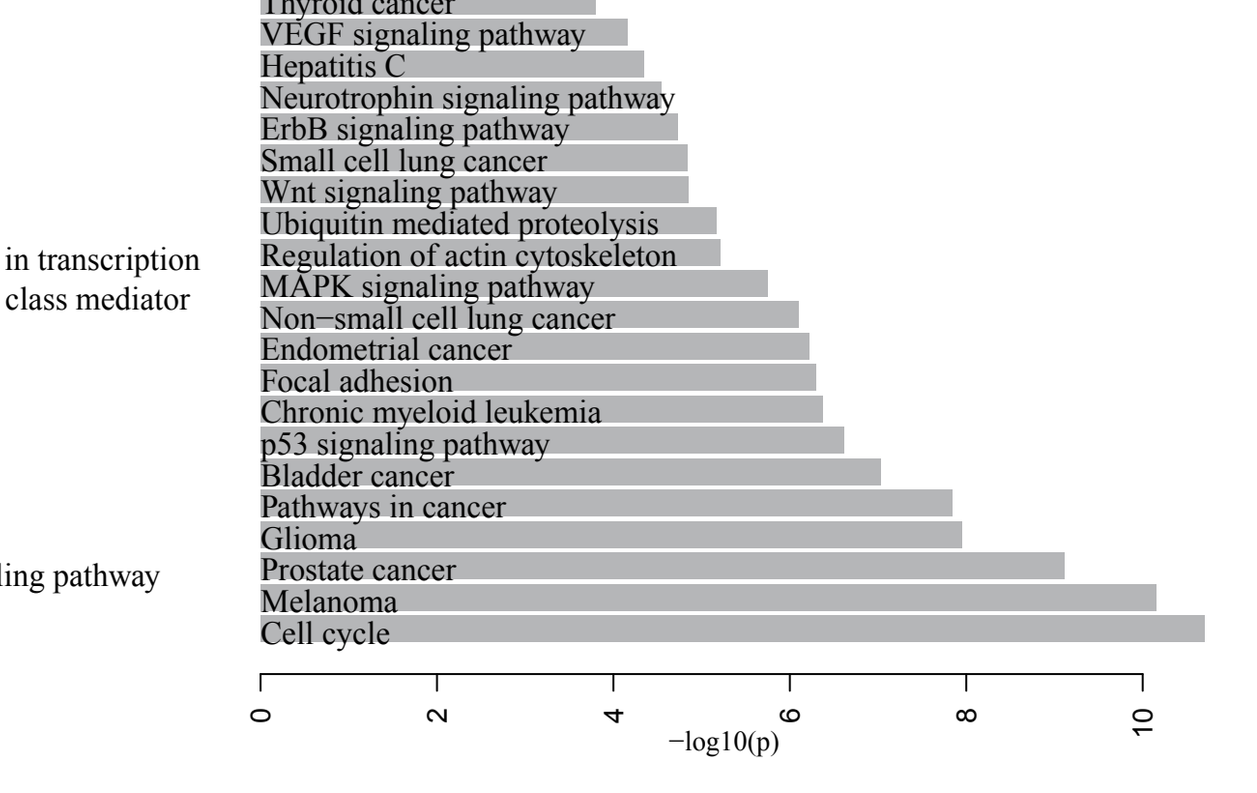

E

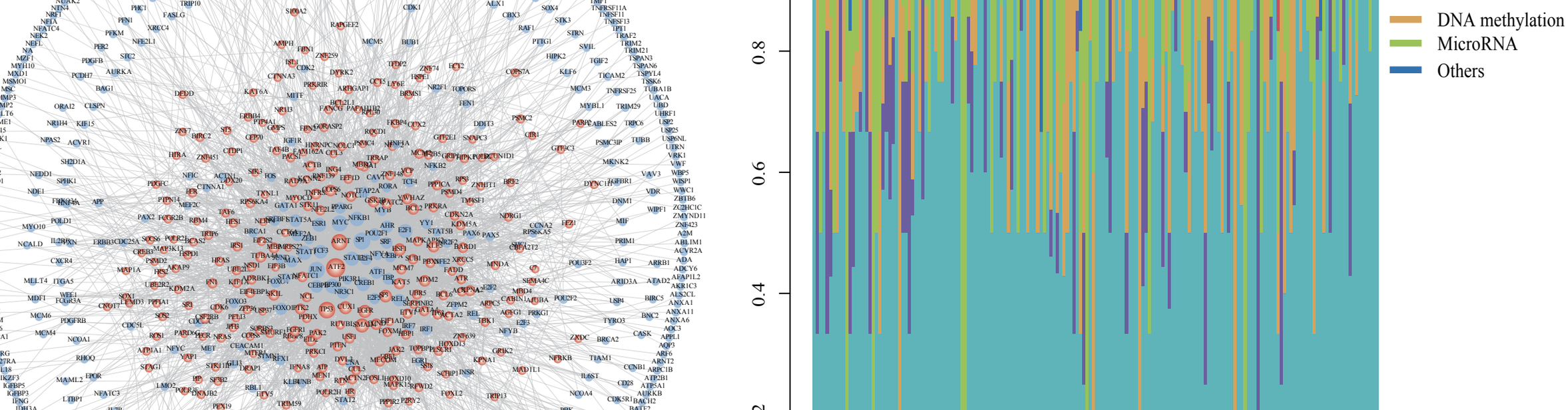

Supplementary Figure S11

A

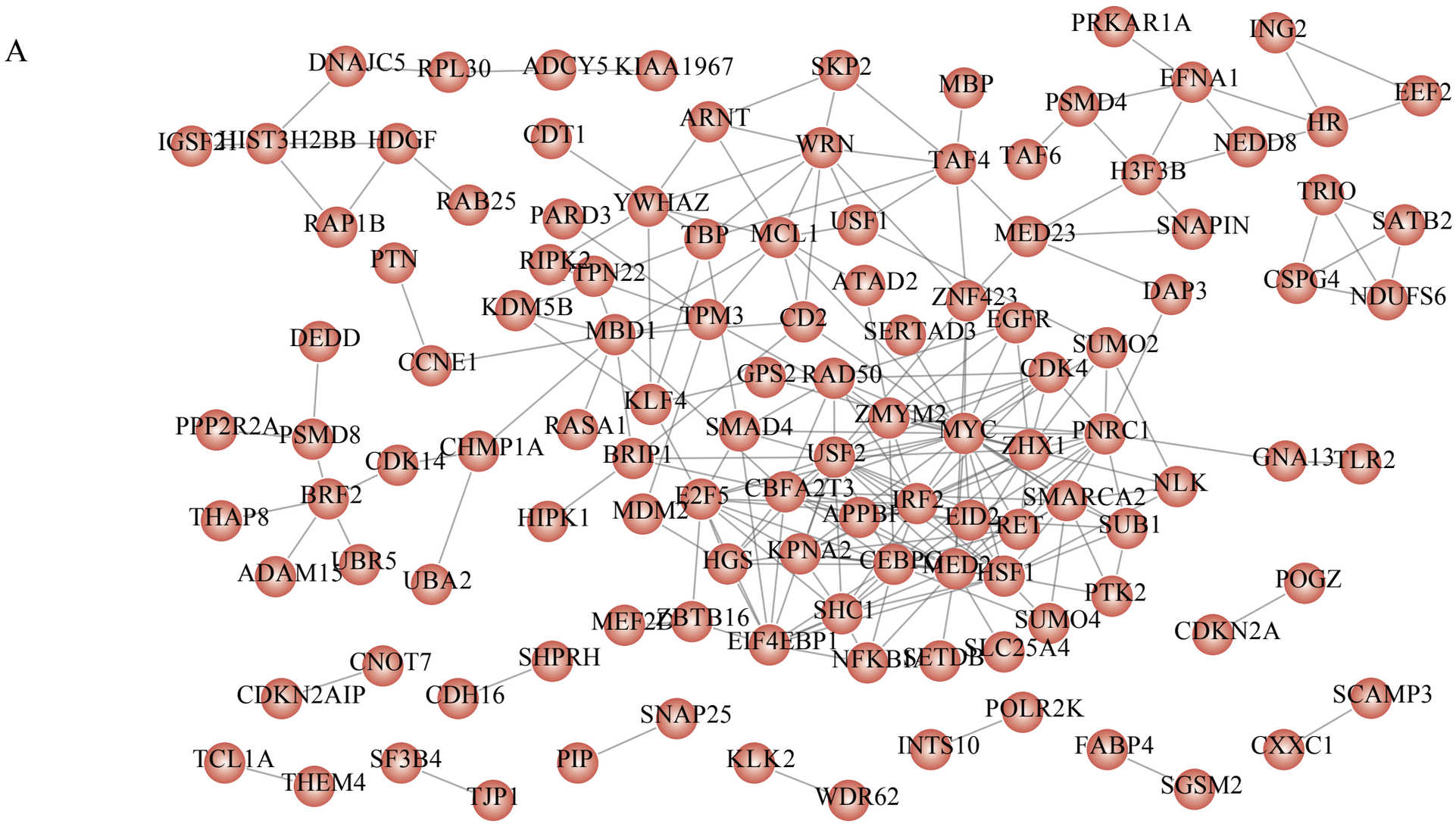

B

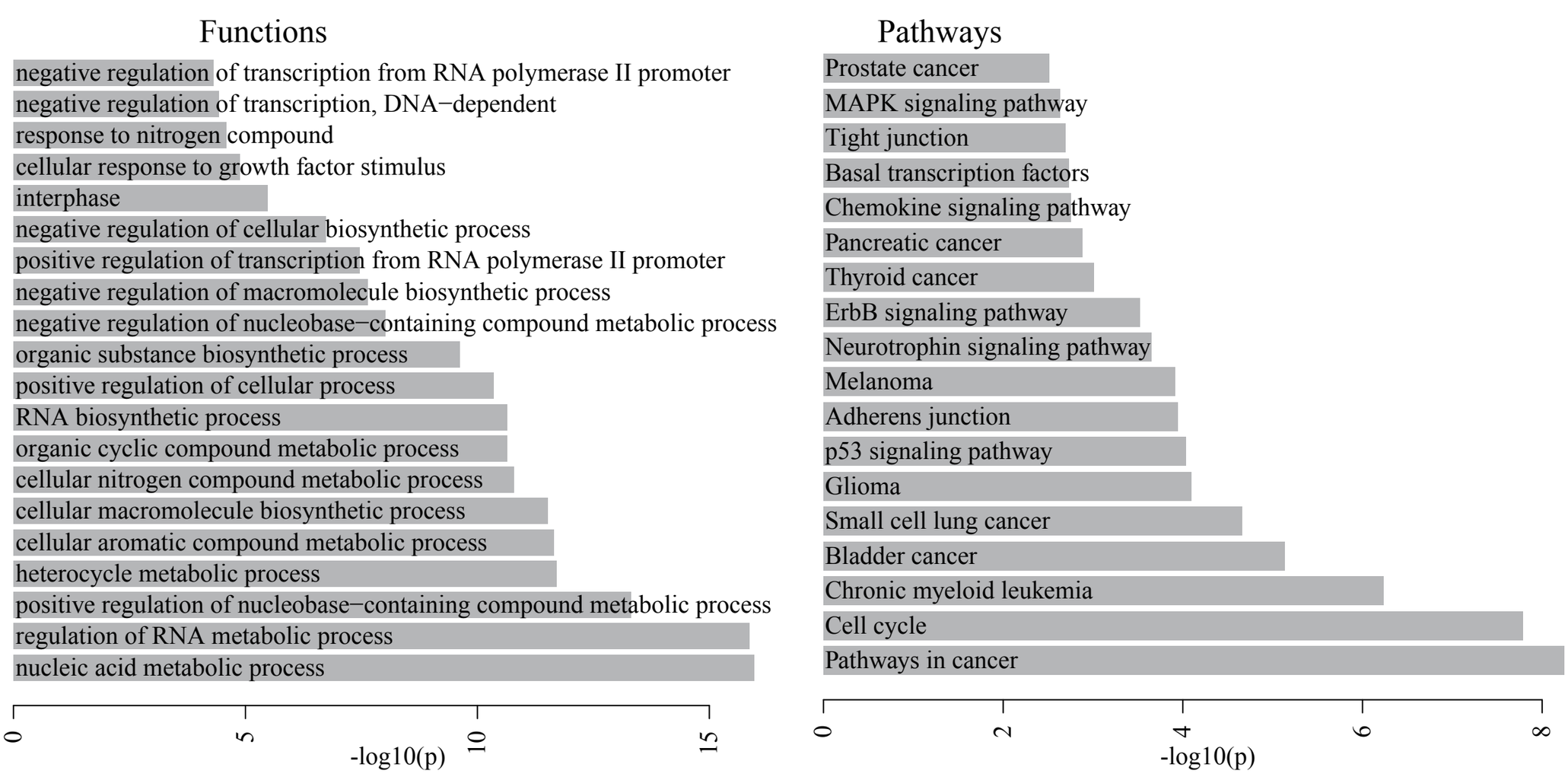

C

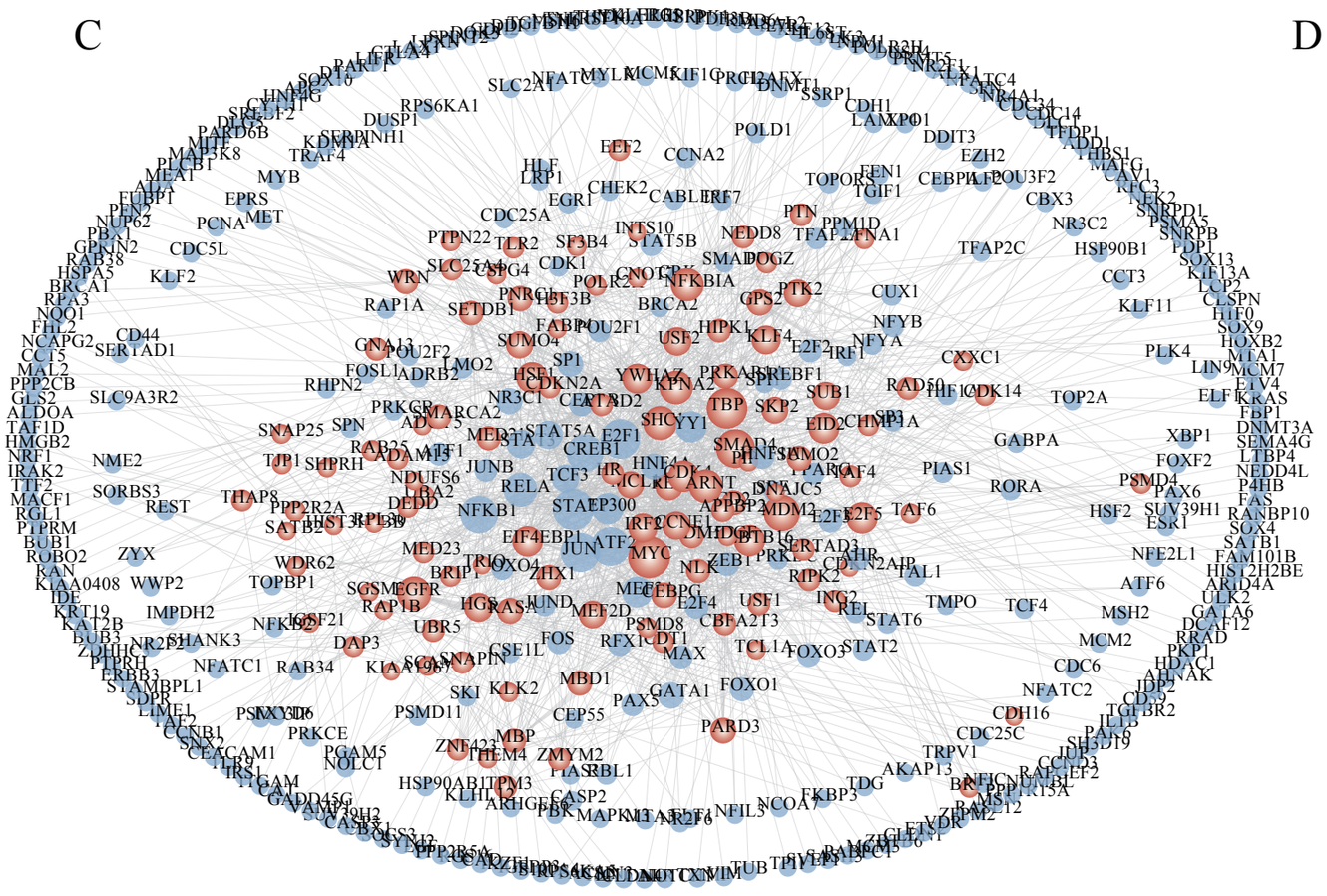

D

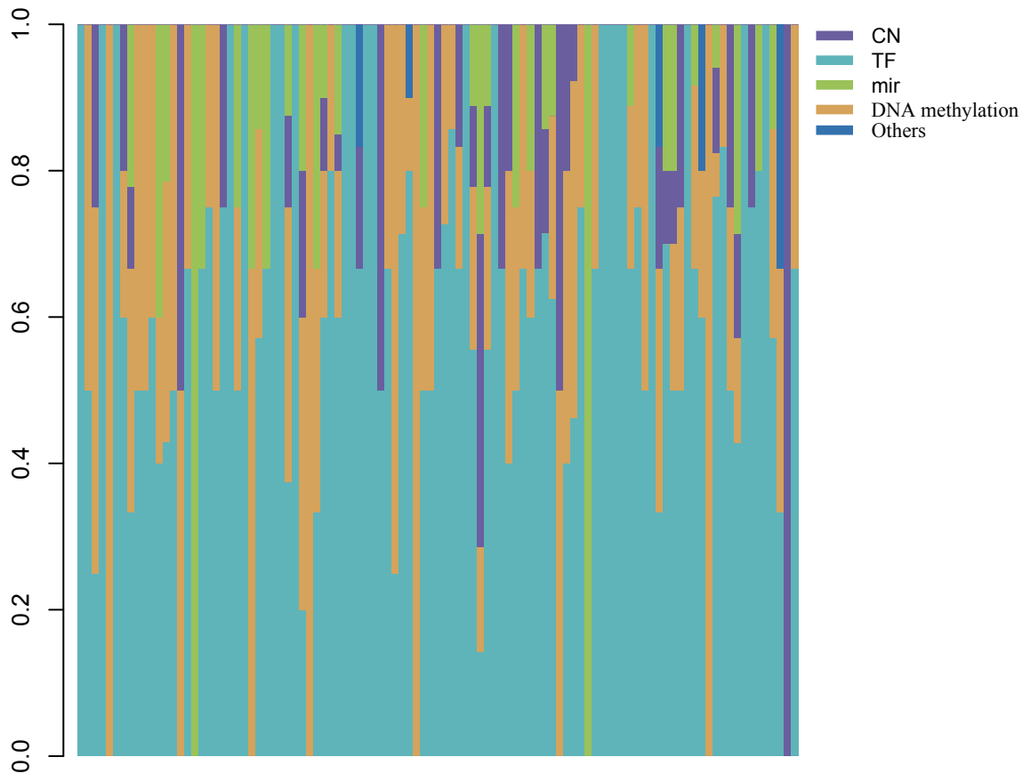

E

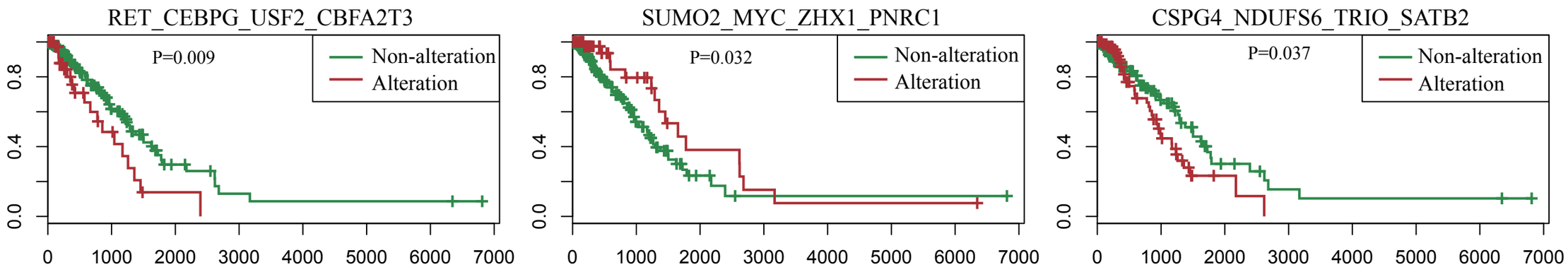

Supplementary Figure S12

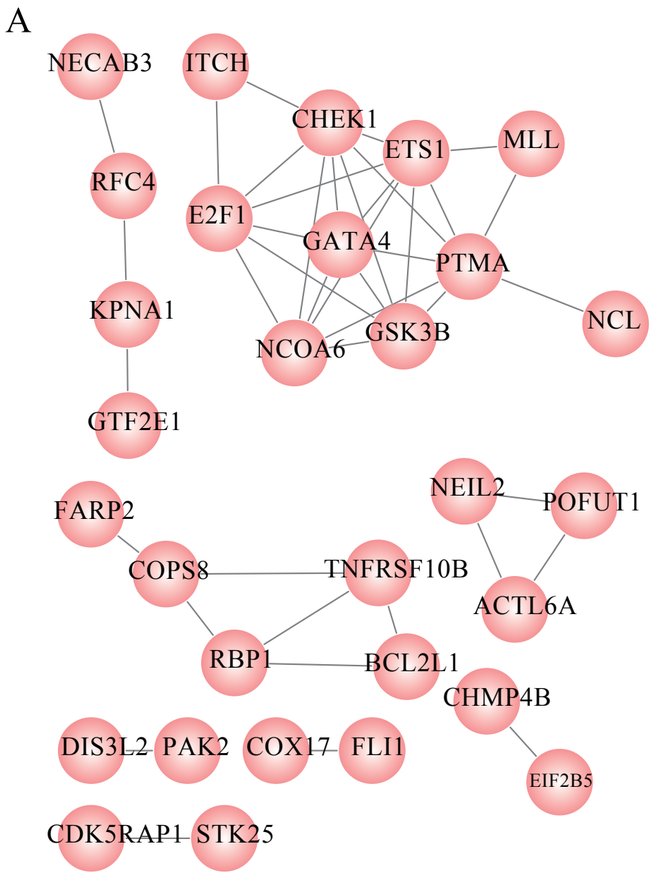

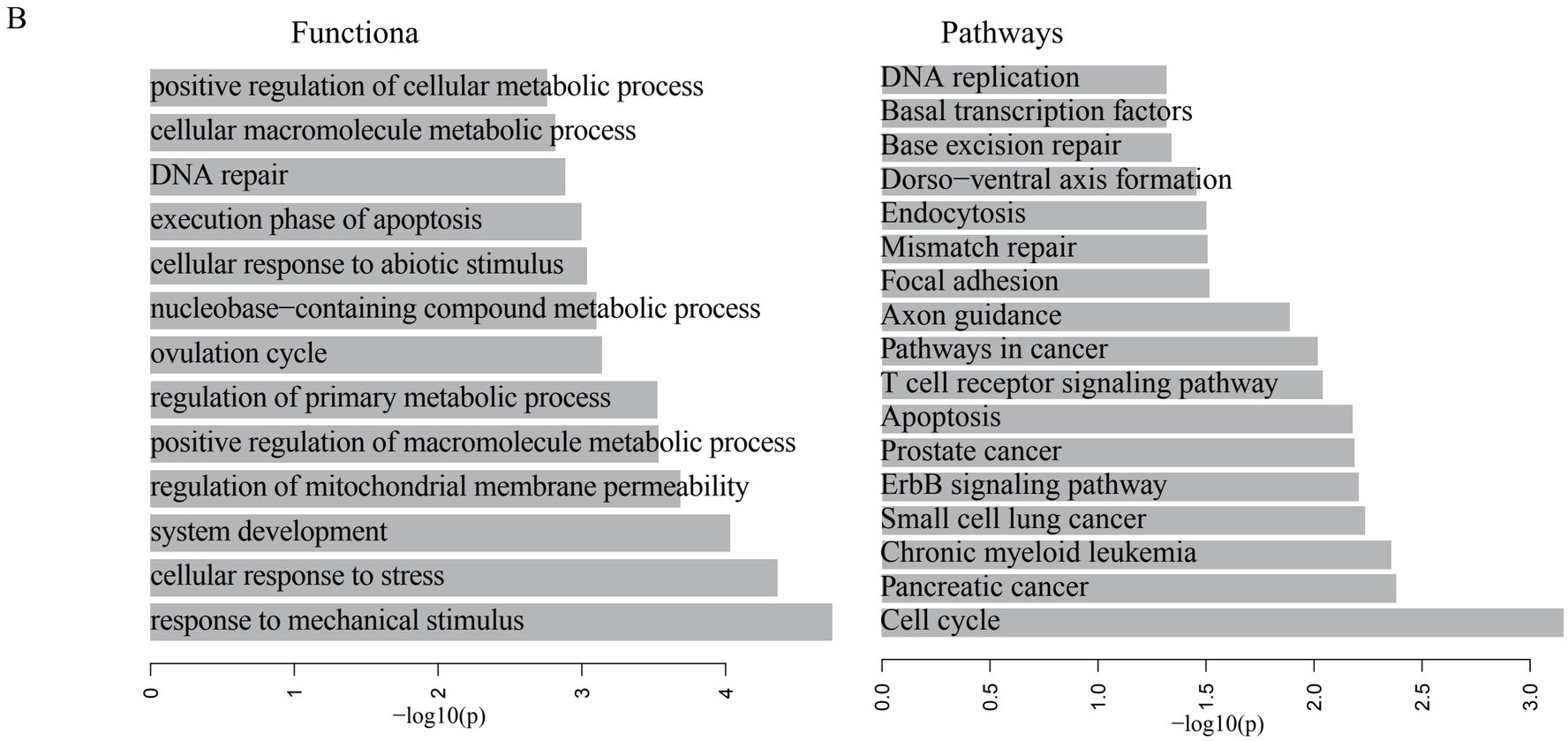

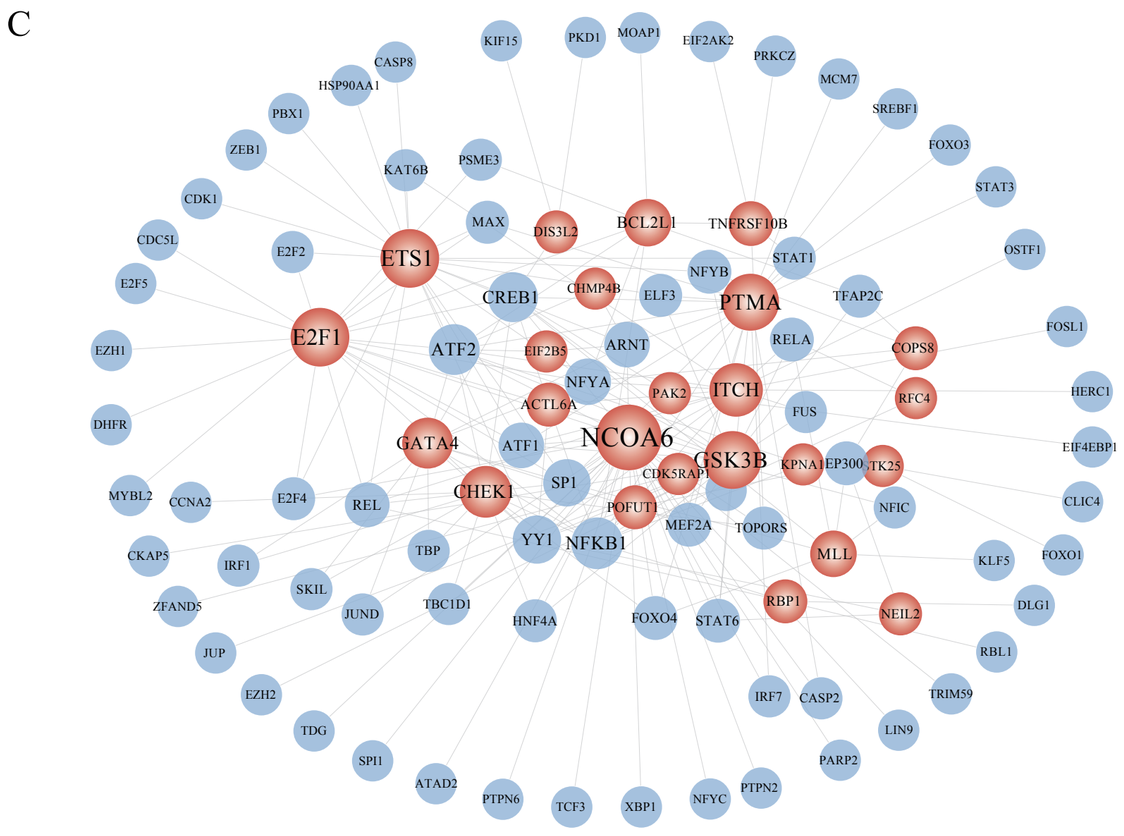

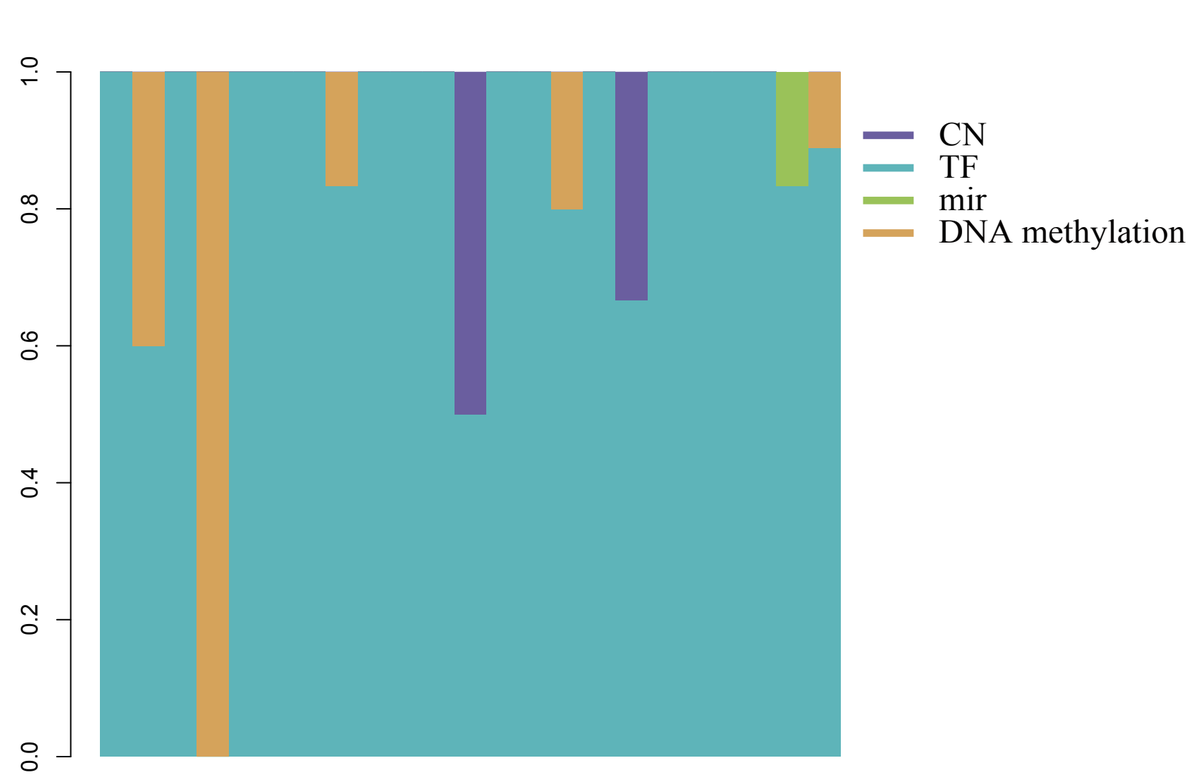

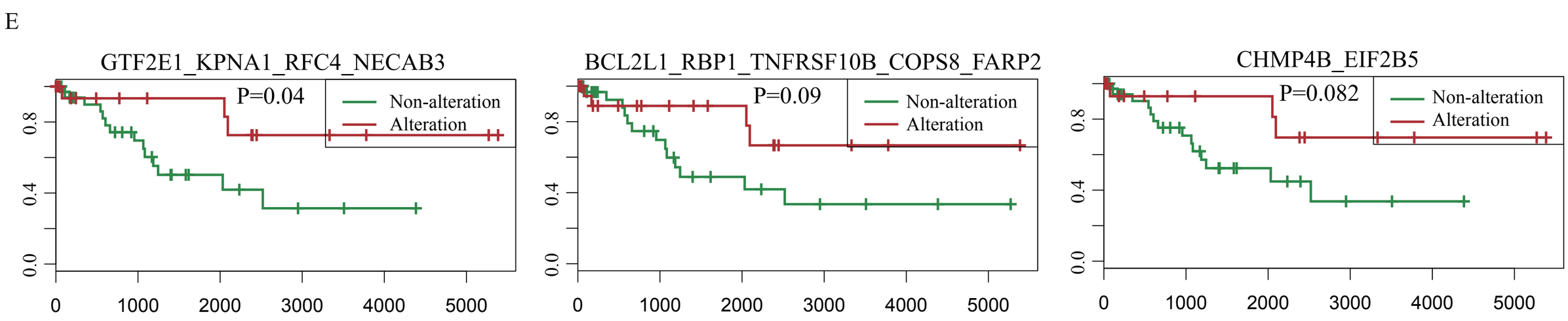

Supplementary Figure S13

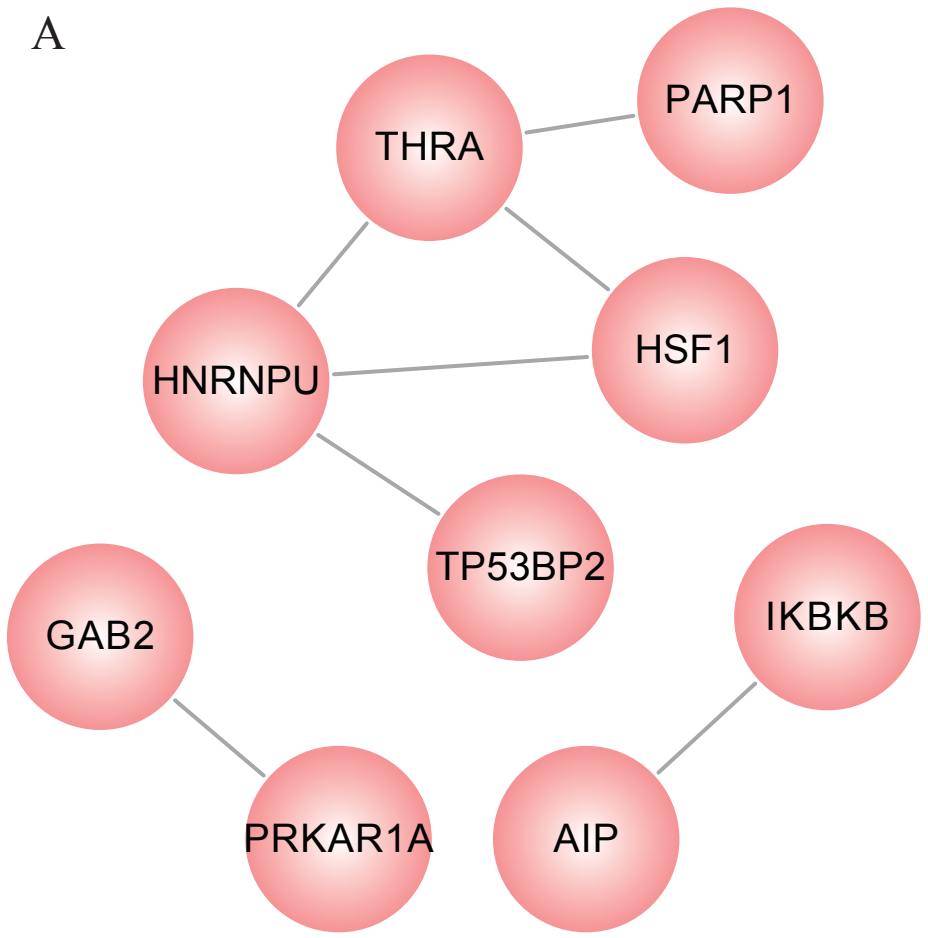

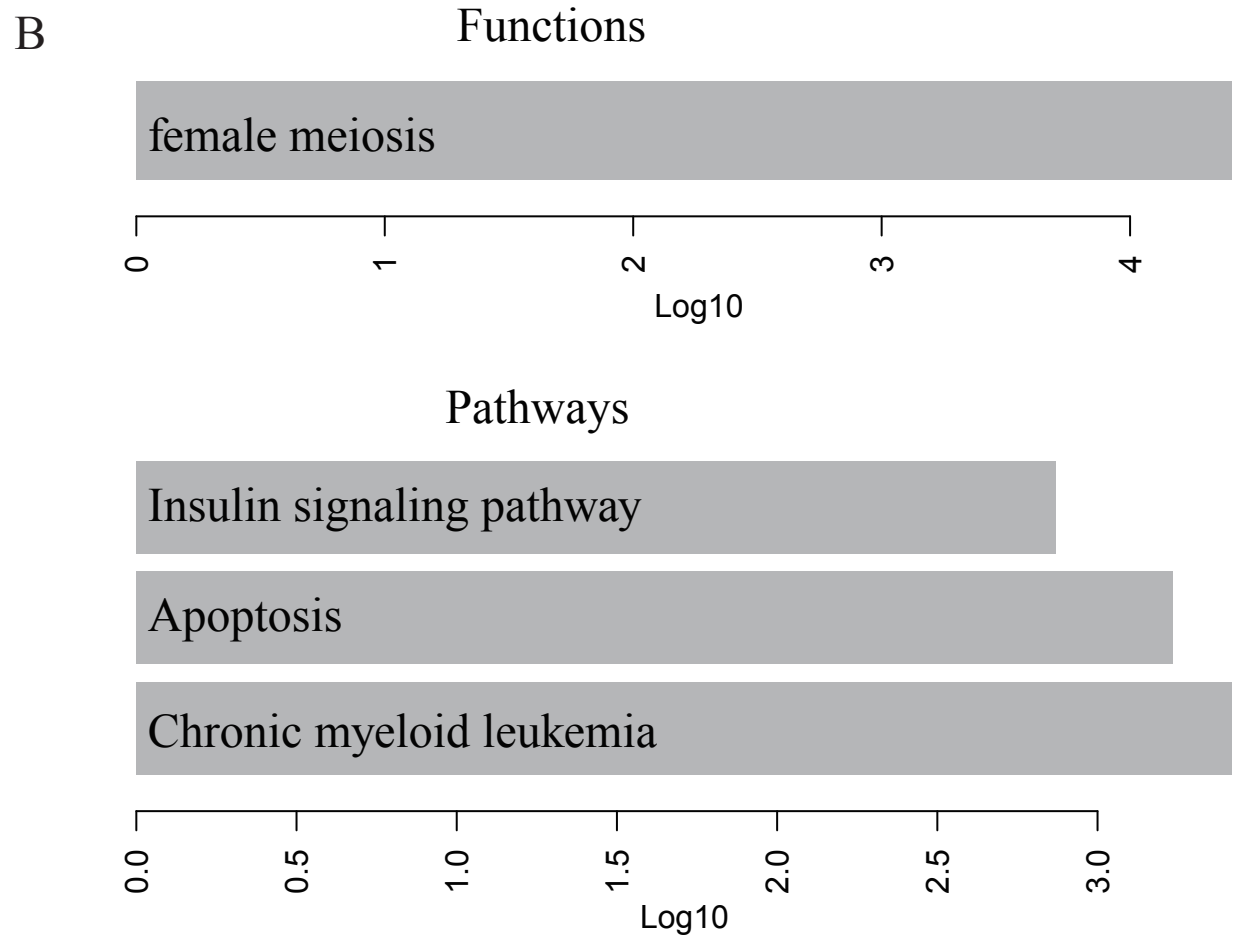

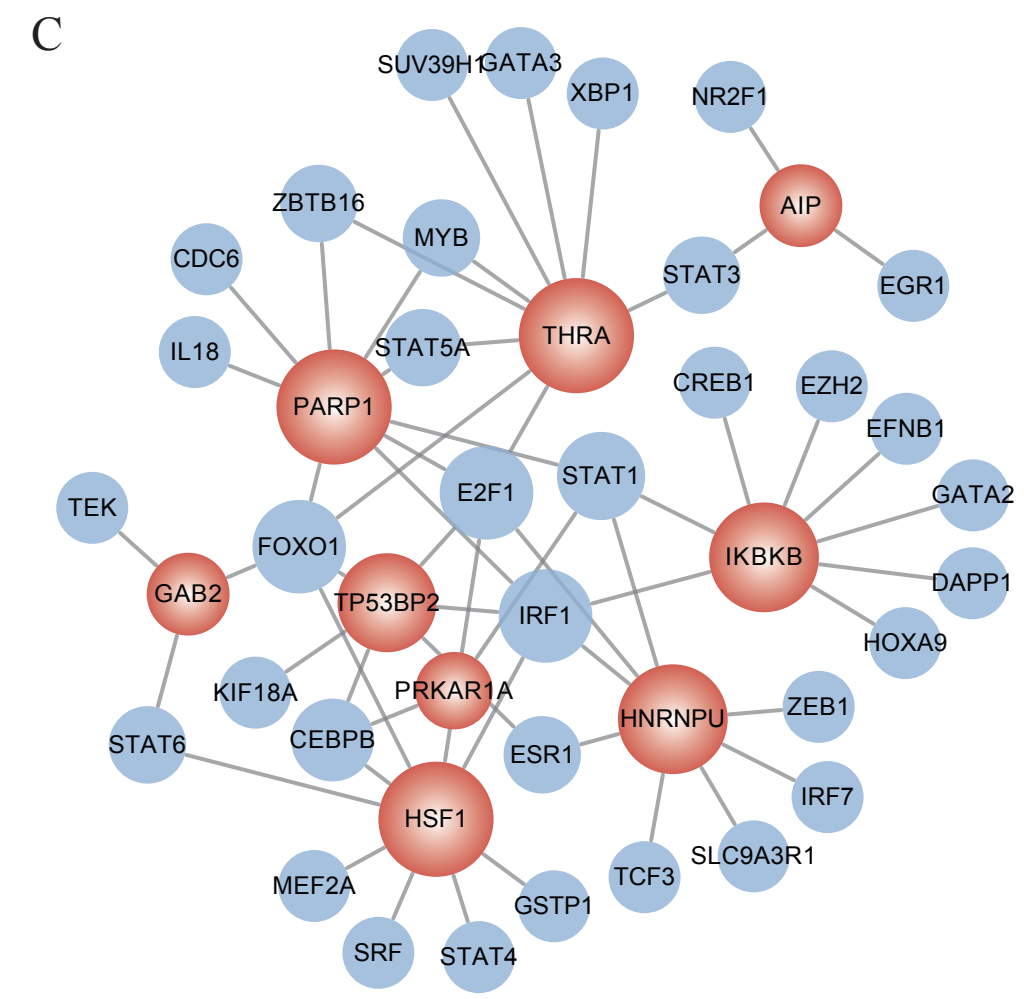

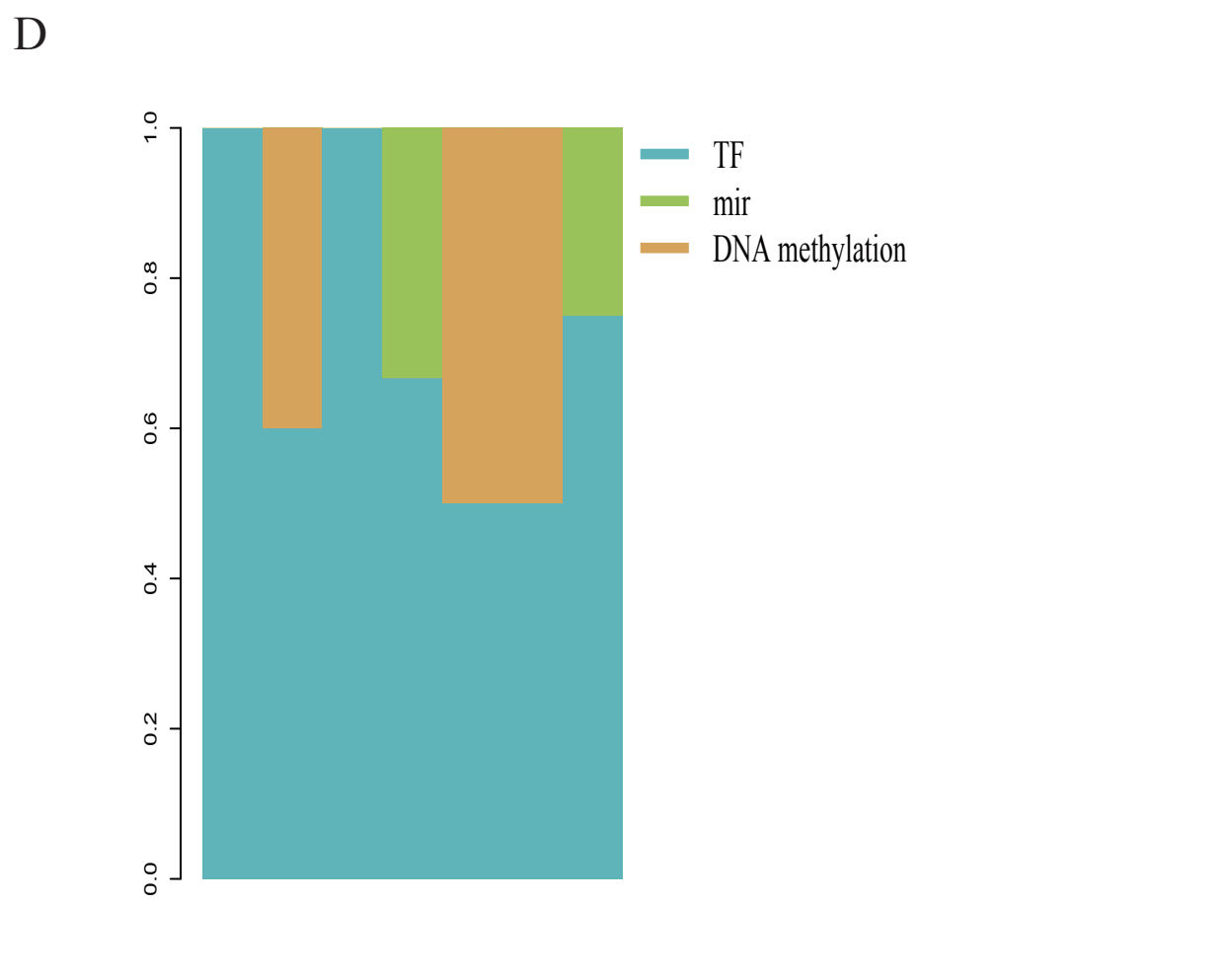

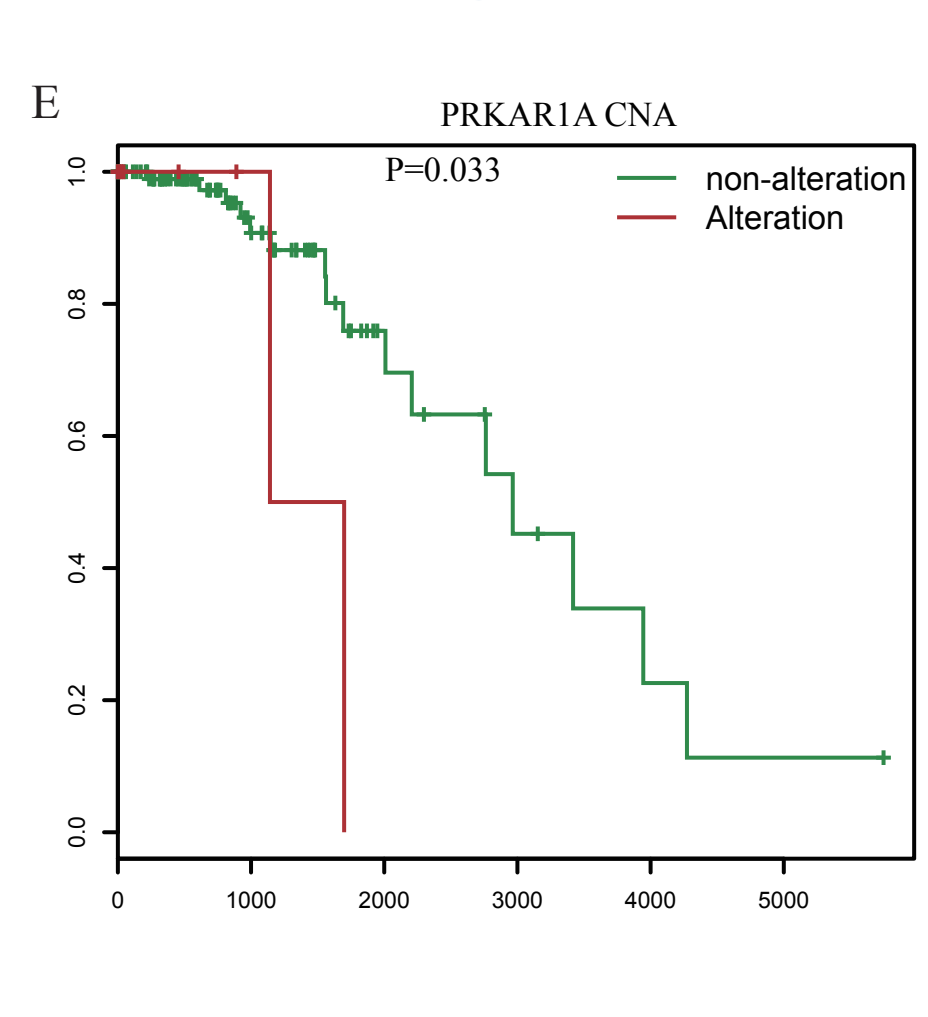

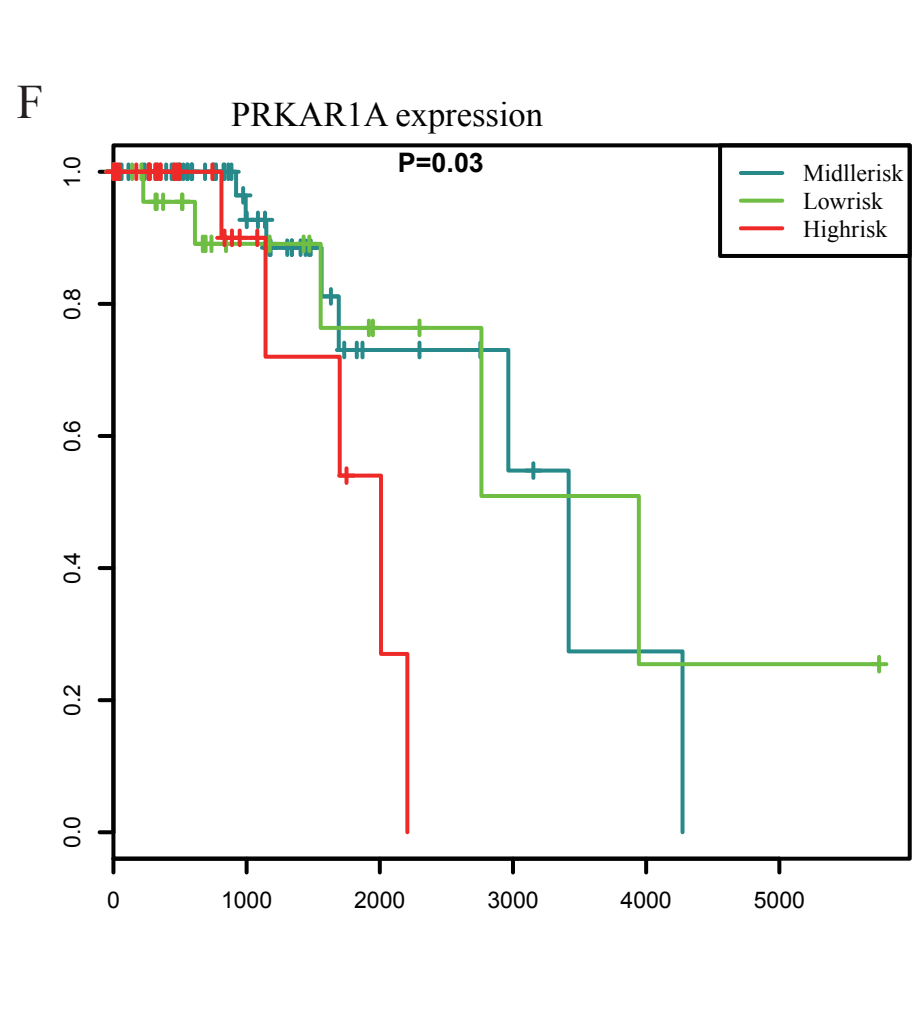

Supplementary Figure S14

A

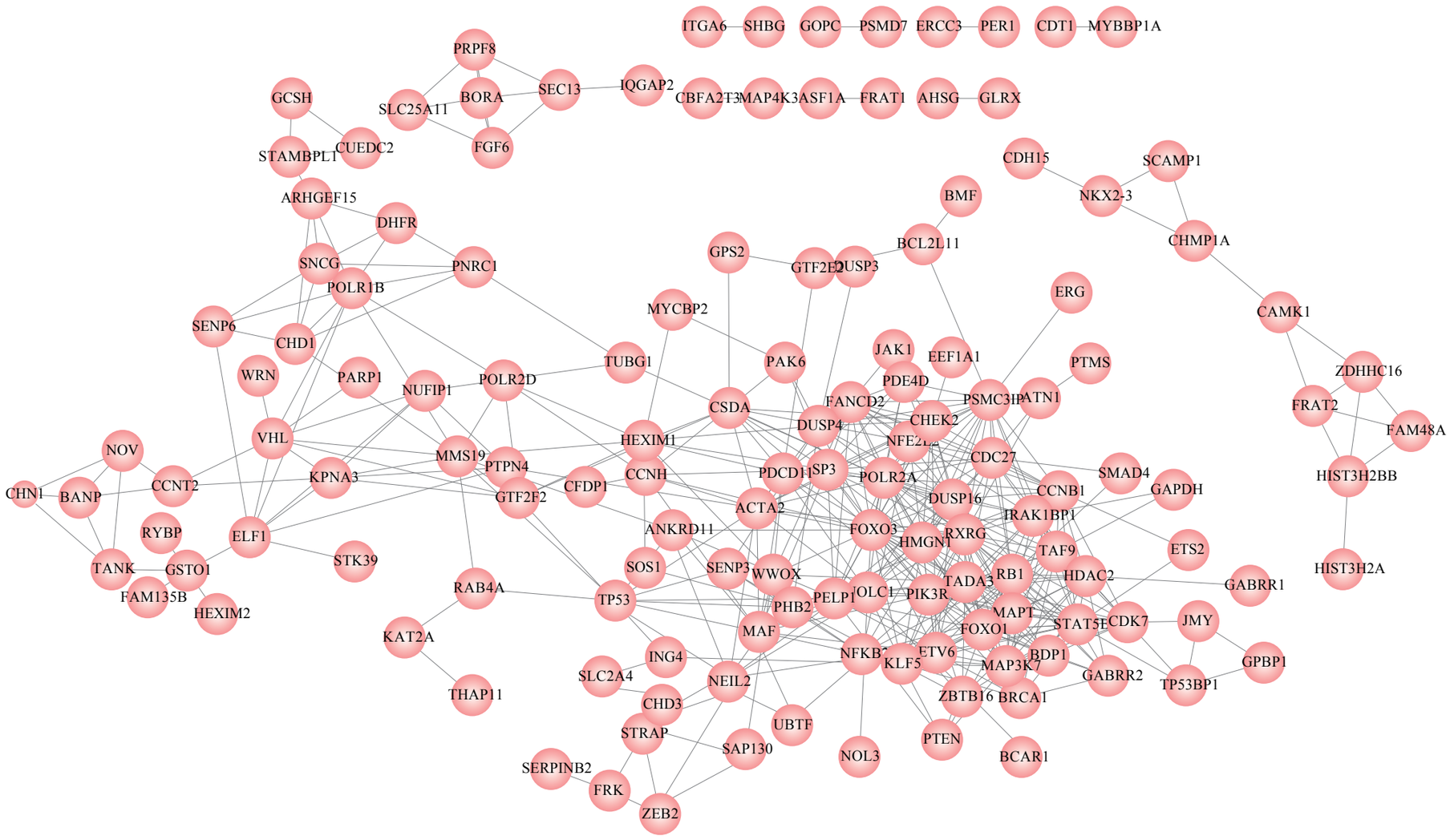

B

Pathways

Apoptosis
Focal adhesion
Type II diabetes mellitus
Nucleotide excision repair
ErbB signaling pathway
Toxoplasmosis
Chemokine signaling pathway
Bladder cancer
Basal transcription factors
Renal cell carcinoma
p53 signaling pathway
Adipocytokine signaling pathway
Colorectal cancer
Thyroid cancer
Dorso−ventral axis formation
Insulin signaling pathway
Hepatitis C
Neurotrophin signaling pathway
Notch signaling pathway
Regulation of actin cytoskeleton
RIG−I−like receptor signaling pathway
B cell receptor signaling pathway
Glioma
Acute myeloid leukemia
RNA polymerase
Wnt signaling pathway
T cell receptor signaling pathway
Adherens junction
Small cell lung cancer
Non−small cell lung cancer
Endometrial cancer
Melanoma
Pancreatic cancer
Prostate cancer
Chronic myeloid leukemia
MAPK signaling pathway
Cell cycle
Pathways in cancer

0 2 4 6 8 10 12 14

-log10(p)

Functions

negative regulation of protein kinase activity
interphase
histone H3 acetylation
positive regulation of viral transcription
negative regulation of transcription from RNA polymerase II promoter
negative regulation of cellular protein metabolic process
Fc−epsilon receptor signaling pathway
transcription−coupled nucleotide−excision repair
neurotrophin TRK receptor signaling pathway
macromolecule modification
positive regulation of cellular process
RNA capping
positive regulation of transcription from RNA polymerase II promoter
7−methylguanosine mRNA capping
transcription elongation from RNA polymerase II promoter
negative regulation of cellular biosynthetic process
negative regulation of nucleobase−containing compound metabolic process
negative regulation of macromolecule biosynthetic process
transcription initiation from RNA polymerase I promoter
termination of RNA polymerase I transcription
transcription initiation from RNA polymerase II promoter
transcription elongation from RNA polymerase I promoter
organic substance biosynthetic process
positive regulation of nitrogen compound metabolic process
regulation of biosynthetic process
cellular nitrogen compound metabolic process
organic cyclic compound metabolic process
heterocycle metabolic process
cellular aromatic compound metabolic process
nucleobase−containing compound biosynthetic process

0 5 10 15

-log10(p)

C

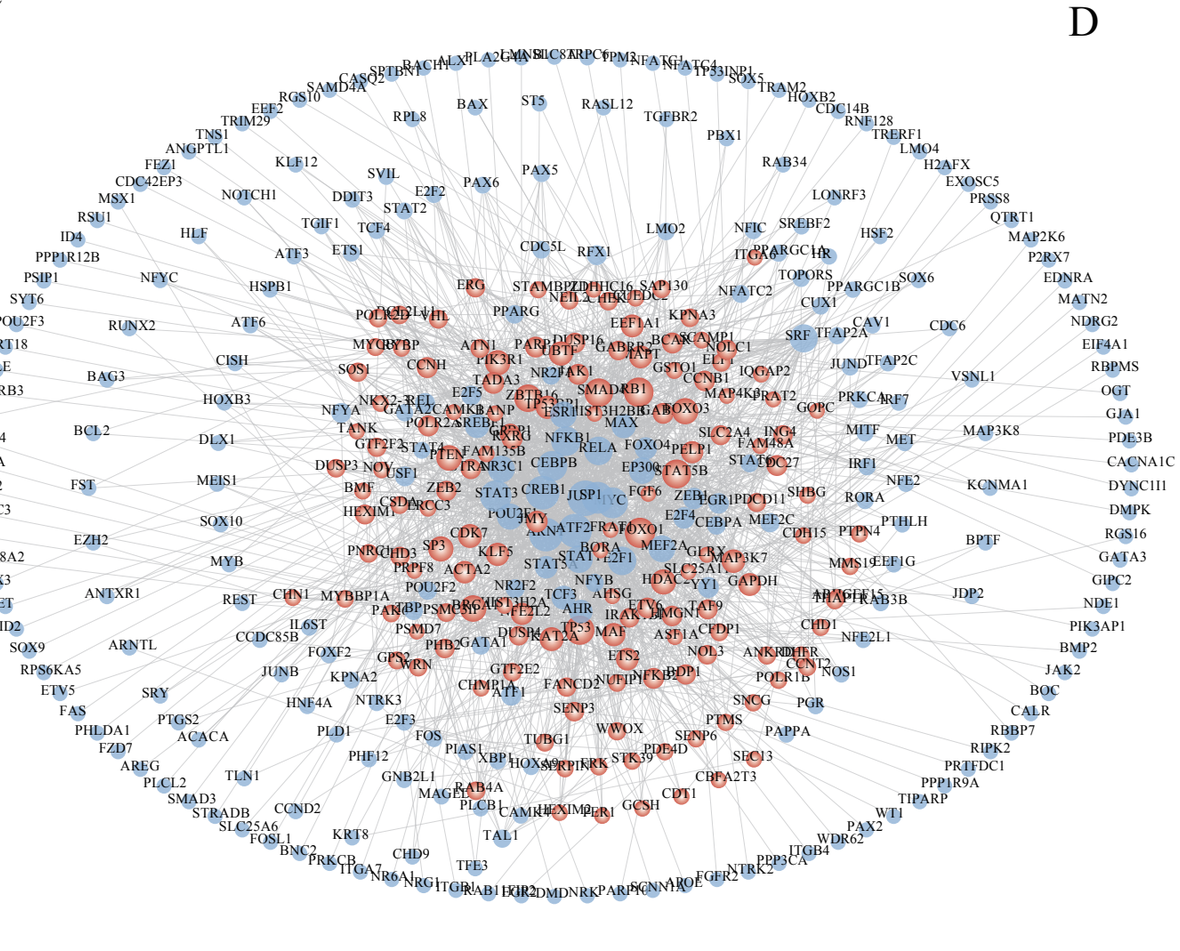

D

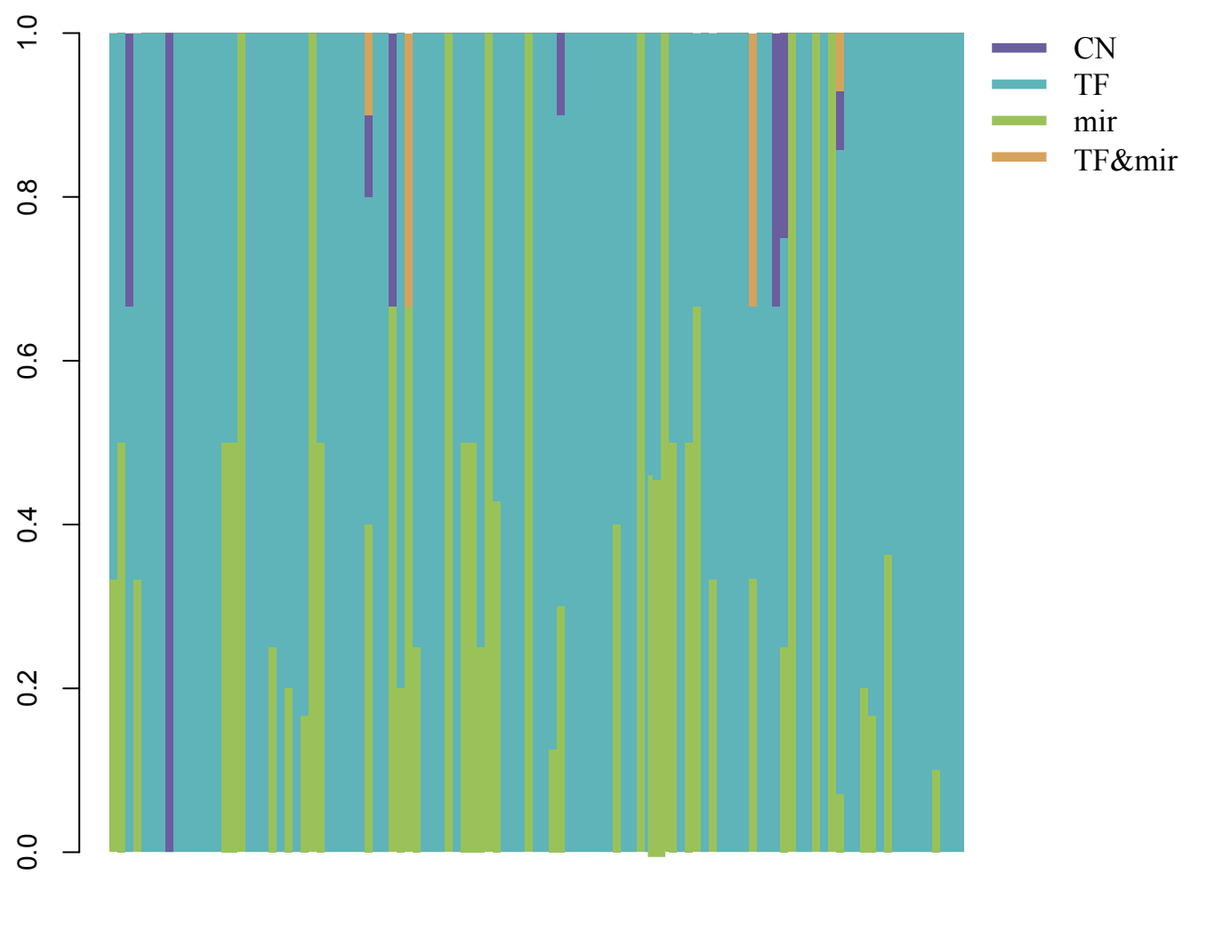

Supplementary Figure S15

A

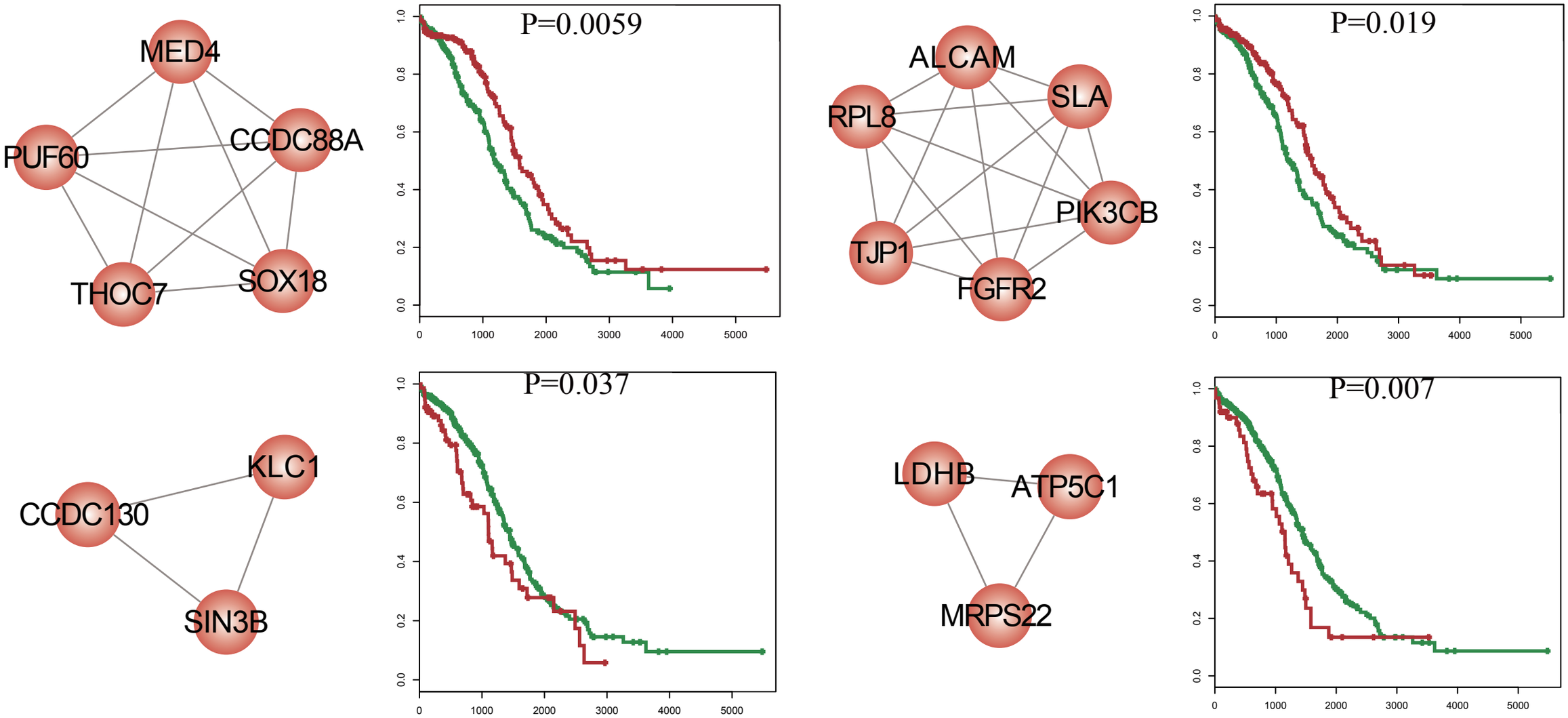

B

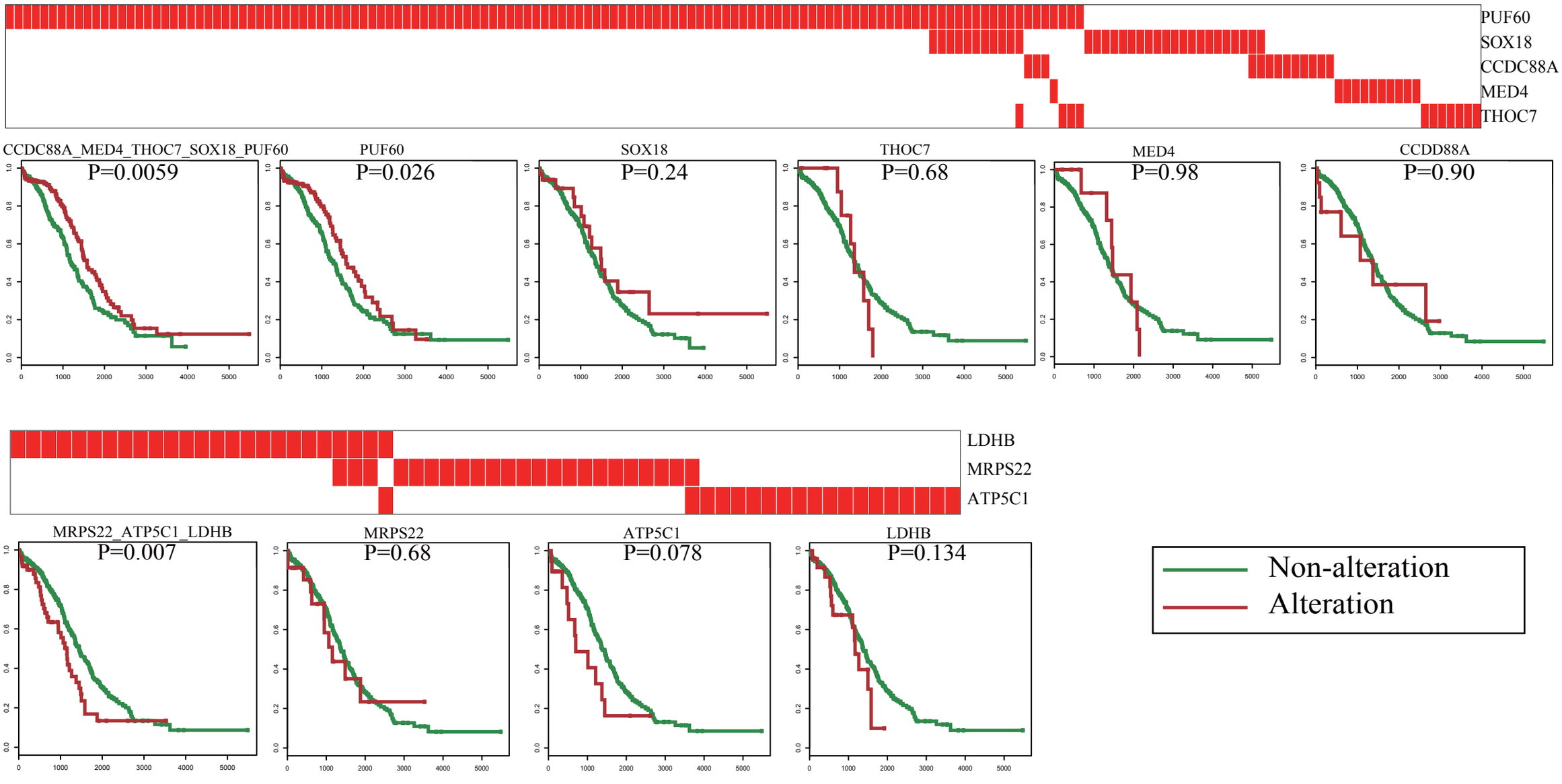

Supplementary Figure S16

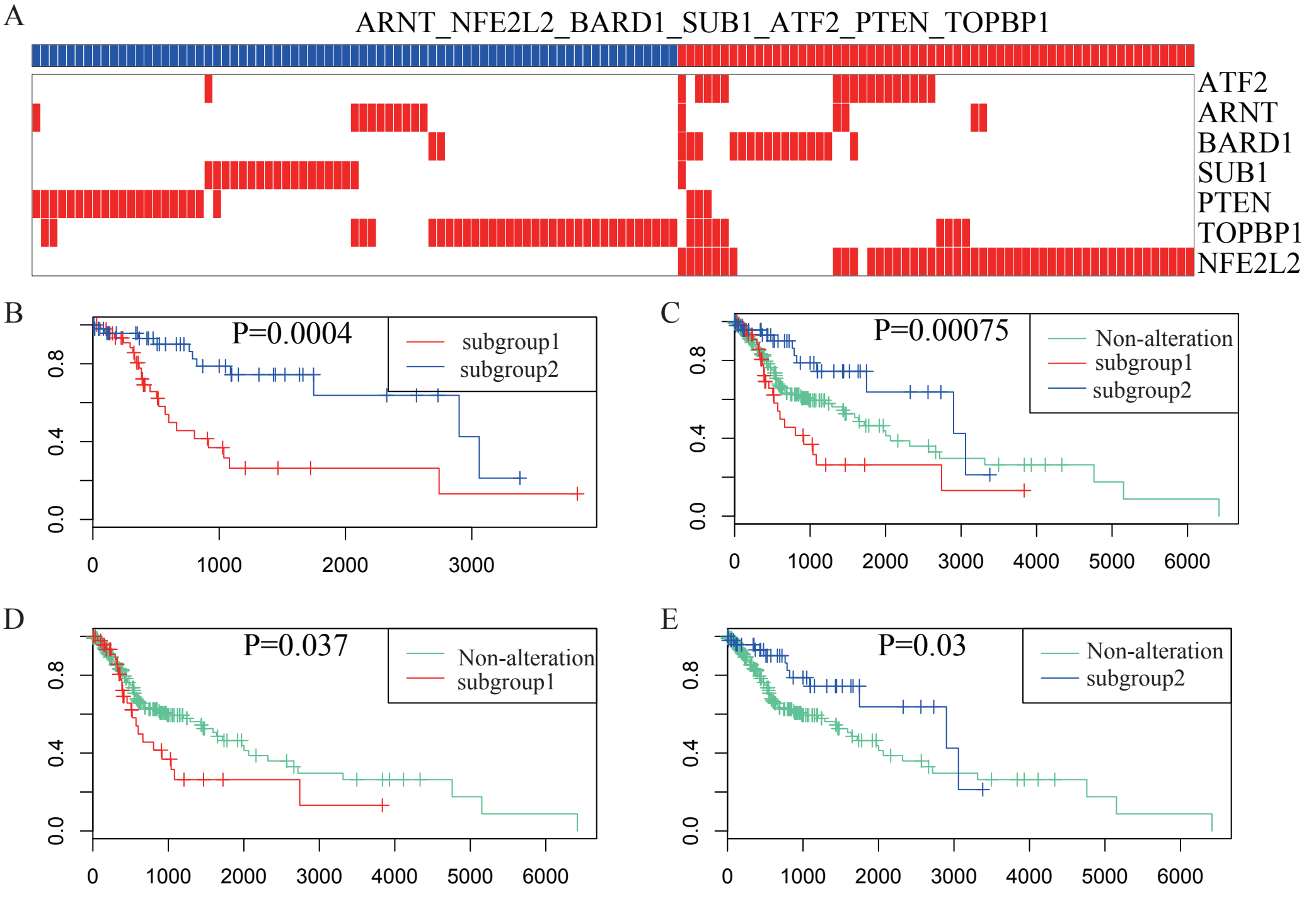

Supplementary Figure S17

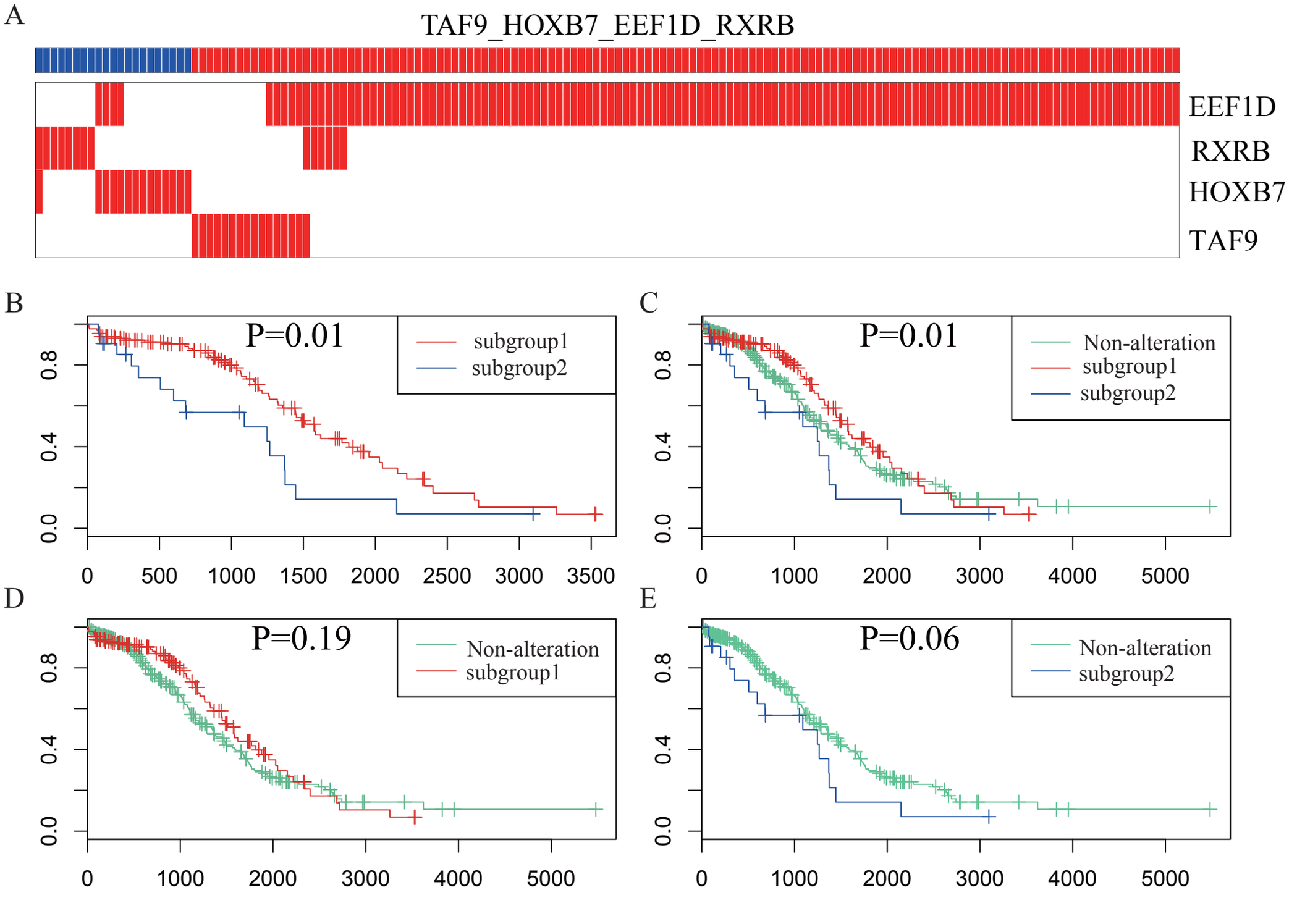

Supplementary Figure S18

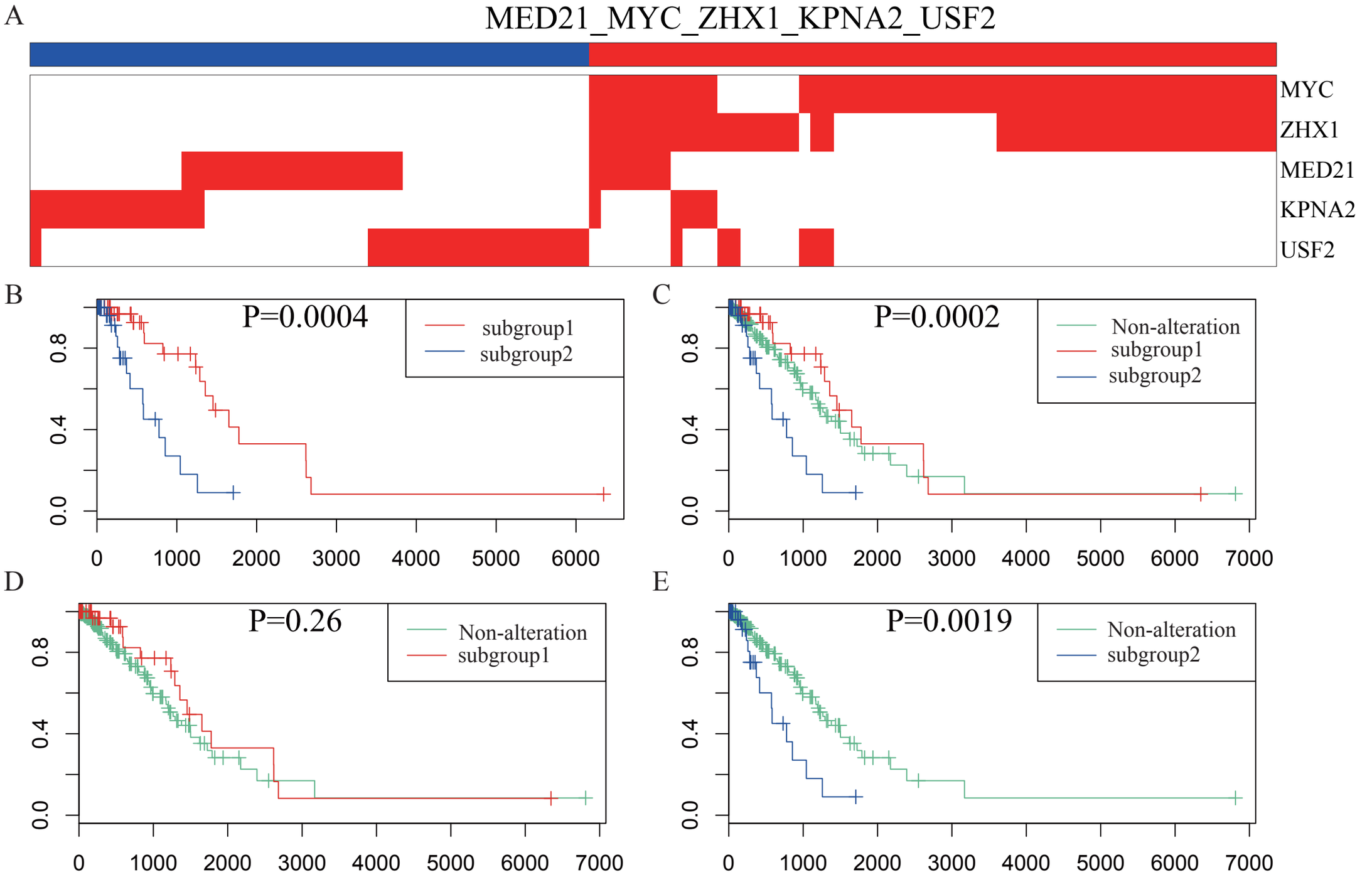

Supplementary Figure S19

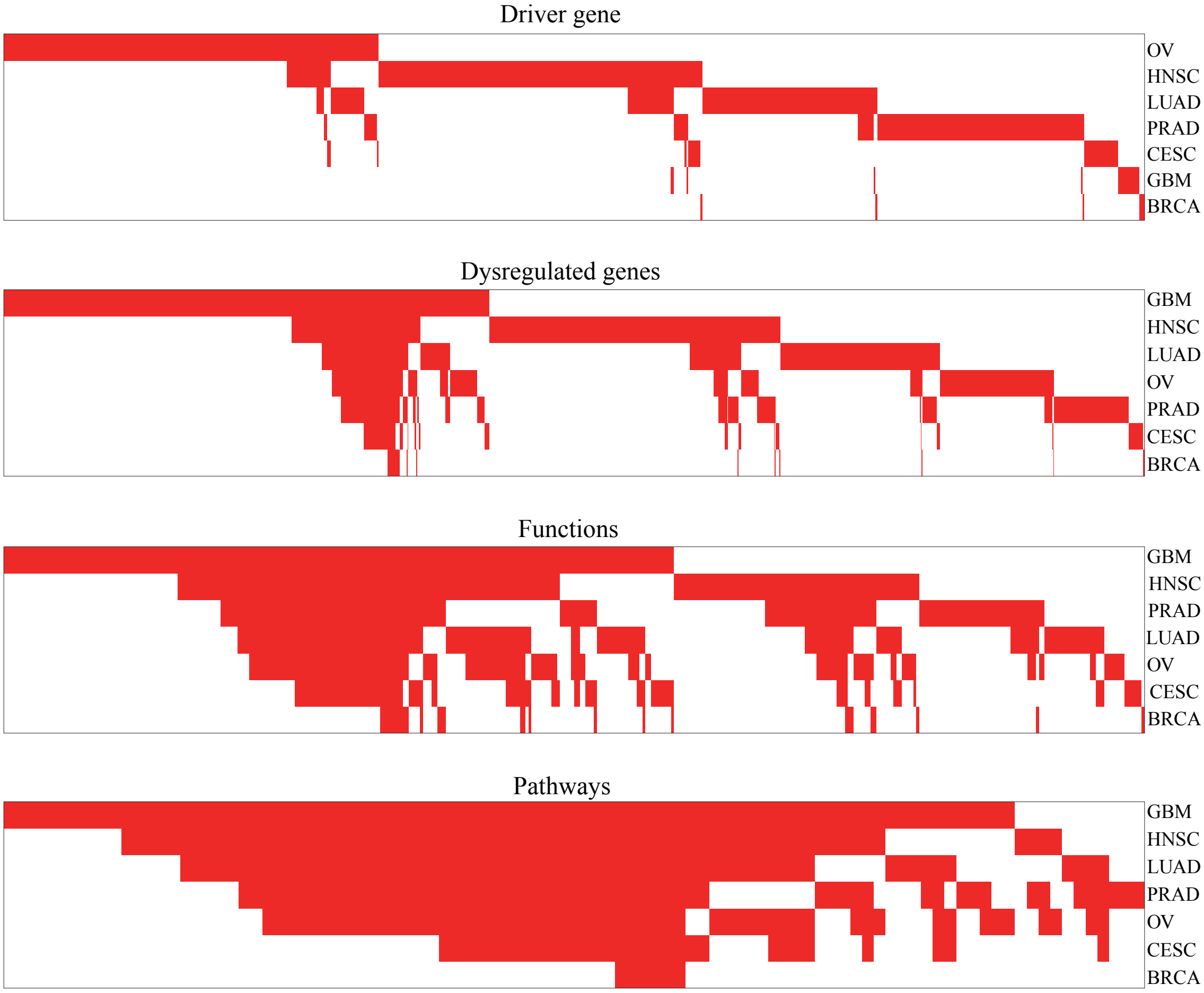

Supplementary Figure S20

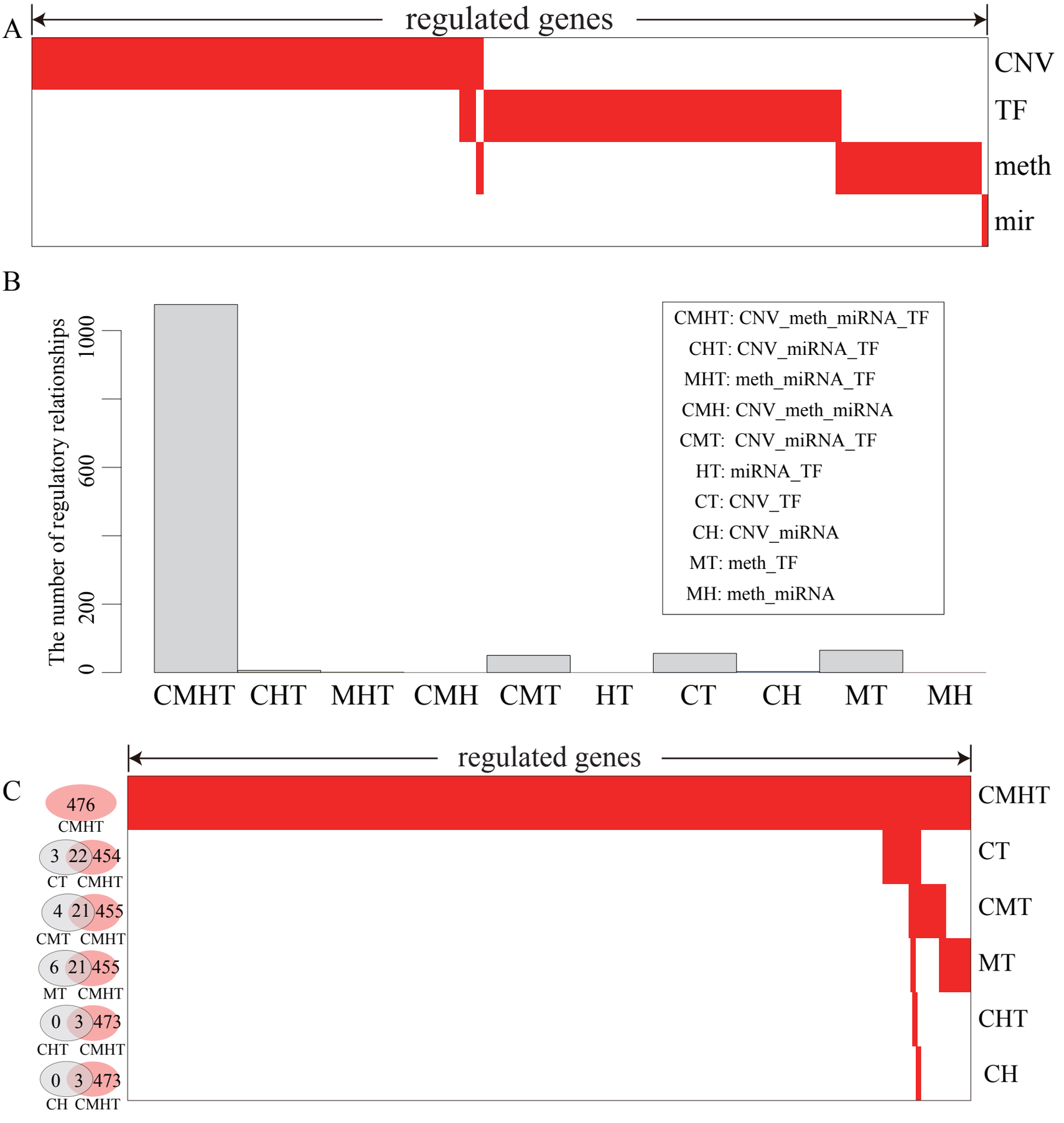

Supplementary Figure S21

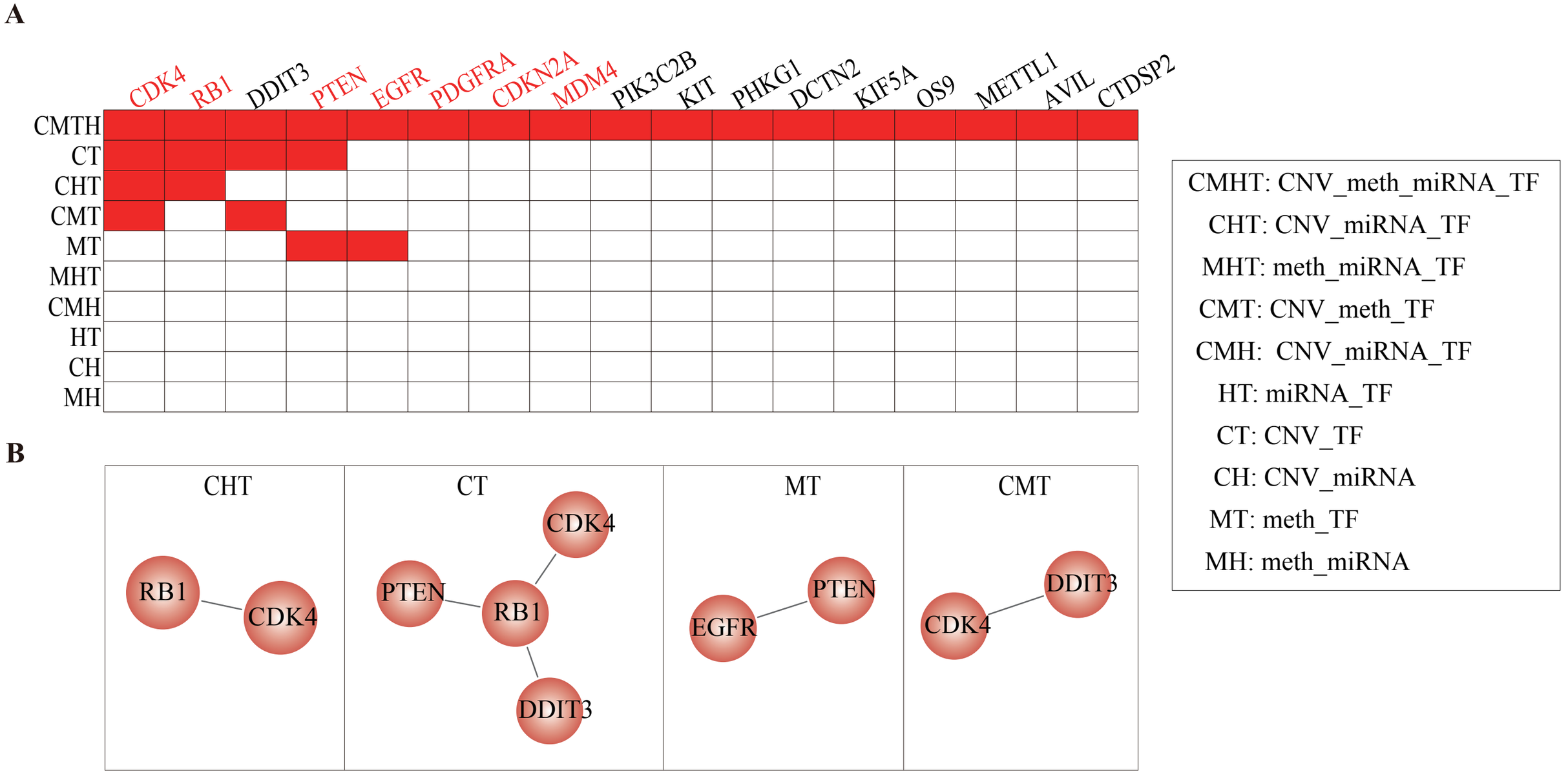

Supplementary Table S1 The information of dysregulated networks for candidate genes

Gene name	Gene num	Tf num	Mir num	Interaction num	CnvGene num	MethGene num	TfGene num	MirGene num
AVIL	1231	114	38	1664	489	144	972	59
B4GALNT1	1300	110	48	1735	531	155	982	67
CCT6A	1194	102	44	1584	497	151	876	60
CDK4	1207	114	36	1621	473	144	950	54
CDKN2A	620	89	17	799	233	59	489	18
CDKN2B	551	86	21	719	205	57	433	24
CHCHD2	1193	102	44	1583	497	150	876	60
CHIC2	1276	108	47	1718	560	166	920	72
CTDSP2	1265	113	41	1700	518	138	975	69
CYP27B1	1209	107	39	1600	480	140	912	68
DCTN2	1351	111	49	1812	576	152	1010	74
DDIT3	1364	117	52	1827	579	165	1012	71
DTX3	1348	111	49	1811	576	153	1008	74
EGFR	778	103	13	1055	230	74	737	14
ELAVL2	945	94	34	1248	347	118	734	49
GBAS	1118	104	38	1479	458	130	833	58
GLI1	1353	117	51	1828	578	160	1007	83
KIF5A	1350	111	49	1812	576	153	1009	74
KIT	1288	111	45	1709	568	175	897	69
KLHL9	903	95	33	1161	364	116	622	59
LANCL2	638	91	23	793	229	82	442	40
MBD6	1309	109	51	1745	564	164	942	75
MDM4	1355	121	46	1854	537	185	1067	65
METTL1	1210	107	39	1600	480	141	911	68
METTL21B	1217	115	38	1641	480	141	960	60
MLLT3	1263	112	45	1708	463	160	1016	69
MRPS17	1119	104	38	1478	458	131	831	58
MTAP	491	72	21	589	172	56	333	28
NF1	1312	107	44	1790	526	166	1041	57
OS9	1238	110	43	1654	491	141	951	71
PDGFRA	1311	115	42	1772	561	181	972	58
PHKG1	1193	102	44	1582	496	150	876	60
PIK3C2B	1345	117	45	1841	537	186	1050	68
PIP4K2C	1340	113	54	1784	561	153	994	76
PSPH	1114	104	32	1501	451	137	859	54
PTEN	661	84	29	862	171	90	562	39
RB1	1229	108	40	1628	519	153	884	72
RYR3	1440	119	49	1981	575	180	1145	81
SEC61G	625	87	19	789	199	59	498	33
SLC26A10	1308	113	49	1744	543	160	975	66
TSFM	1217	115	38	1641	480	141	960	60

Gene name	Gene num	Tf num	Mir num	Interaction num	CnvGene num	MethGene num	TfGene num	MirGene num
AVIL	1231	114	38	1664	489	144	972	59
TSPAN31	1207	114	36	1621	473	144	950	54
CDK4	1207	114	36	1621	473	144	950	54
CDKN2A	620	89	17	799	233	59	489	18
CTDSP2	1265	113	41	1700	518	138	975	69
DCTN2	1351	111	49	1812	576	152	1010	74
DDIT3	1364	117	52	1827	579	165	1012	71
EGFR	778	103	13	1055	230	74	737	14
KIF5A	1350	111	49	1812	576	153	1009	74
KIT	1288	111	45	1709	568	175	897	69
MDM4	1355	121	46	1854	537	185	1067	65
METTL1	1210	107	39	1600	480	141	911	68
OS9	1238	110	43	1654	491	141	951	71
PDGFRA	1311	115	42	1772	561	181	972	58
PHKG1	1193	102	44	1582	496	150	876	60
PIK3C2B	1345	117	45	1841	537	186	1050	68
PTEN	661	84	29	862	171	90	562	39
RB1	1229	108	40	1628	519	153	884	72

Supplementary Table S2. The datasets for other six types of cancer

Cancer name	Gene expression	miRNA expression	DNA methylation	Copy number	Somaticmutations	Common samples
Ovarian serous cystadenocarcinoma [OV]	HG-U133A (578)	H-miRNA _8x15Kv2 (500)	Methyl27 (613)	SNP_6.0 (570)	SOLiD_DNASeq IlluminaGA_DNASeq IlluminaGA_DNASeq (462)	446
Head and Neck squamous cell carcinoma[HNSC]	IlluminaHiSeq _RNASeqV2 (495)	IlluminaHiSeq _miRNASeq (467)	Methyl450 (516)	SNP_6.0 (509)	IlluminaGA_DNASeq IlluminaGA_DNASeq_automated (511)	437
Lung adenocarcinoma [LUAD]	IlluminaHiSeq _RNASeqV2 (488)	IlluminaHiSeq _miRNASeq (428)	Methyl450 (450)	SNP_6.0 (494)	IlluminaGA_DNASeq (519)	389
Cervical squamous cell carcinoma and endocervical adenocarcinoma [CESC]	IlluminaHiSeq _RNASeqV2 (185)	IlluminaHiSeq _miRNASeq (200)	Methyl450 (211)	SNP_6.0 (192)	IlluminaGA_DNASeq IlluminaGA_DNASeq_automated (324)	180
Breast invasive carcinoma[BRCA]	AgilentG4502 A_07_3 (529)	IlluminaHiSeq _miRNASeq (782)	Methyl27 (342)	SNP_6.0 (911)	IlluminaGA_DNASeq IlluminaGA_DNASeq_curated (519)	131
Prostate adenocarcinoma [PRAD]	IlluminaHiSeq _RNASeqV2 (297)	IlluminaHiSeq _miRNASeq (326)	Methyl450 (340)	SNP_6.0 (331)	IlluminaGA_DNASeq IlluminaGA_DNASeq_automated IlluminaGA_DNASeq_automated IlluminaGA_DNASeq_curated (300)	284